

CELLULAR AND MOLECULAR ASPECTS OF ARM REGENERATION IN BRITTLE STARS

ANGELA P. DUQUE-ALARCON

DOTTORATO DI RICERCA IN
BIOLOGIA ANIMALE-XXVII CICLO



UNIVERSITÀ DEGLI STUDI DI MILANO SCUOLA DI
DOTTORATO IN IN TERRA, AMBIENTE, BIODIVERSITÀ
DOTTORATO DI RICERCA IN BIOLOGIA ANIMALE

Docenti Guida: Prof.ssa M.D. CANDIA CARNEVALI
Prof. LUCA DEL GIACCO

Coordinatore del Dottorato: Prof. C. Bandi

Tesi di Dottorato svolta presso il Dipartimento di Bioscienze dell'Università degli
Studi di Milano, via Celoria 26, Milano.

ANNO ACCADEMICO 2014-2015
© Copyright 2015, Angela P. Duque-Alarcon

Dedication: To Fabi. Thank you for holding me.

Table of Contents

	Page
Abstract	7
List of Tables	9
List of Figures	10
1. Introduction	11
1.1 The phylum Echinodermata	11
1.1.1. Echinoderm bauplan and general features	11
1.1.2. Ophiuroid distinctive features	13
1.2. Regeneration	15
1.2.1. Regeneration in animal biology	15
1.2.2. The explants and double explants	18
1.2.3. Regenerative mechanisms and model systems	20
1.2.4. Regeneration at cellular and tissue level	21
1.2.5. Regeneration in Ophiuroids	22
1.3. The experimental models	24
1.3.1. <i>Ophioderma longicauda</i> : general features	24
1.3.1.1. <i>Ophioderma longicauda</i> : arm anatomy	25
1.3.2. <i>Amphiura filiformis</i> : general features	26
1.3.3. <i>Ophioderma appressa</i> : general features	26
1.3.4. <i>Ophioderma cinerea</i> : general features	27

2. Objectives	28
3. Materials and methods	29
3.1. <i>Ophioderma longicauda</i>	29
3.1.1. Animal collection and stabling conditions	29
3.1.2. Regeneration experiments	29
3.1.2.1. Morphological and histological analysis	29
3.1.2.1.1. Scanning electron microscopy (SEM) in whole arms	29
3.1.2.1.2. SEM in sectioned arms	30
3.1.2.2. Molecular biology experiments	30
3.1.2.2.1. RNA extraction	31
3.1.2.2.2. Suppressive Subtraction Hybridization (SSH) library	31
3.1.2.2.3. cDNA synthesis and Rsa I digestion	31
3.1.2.2.4. Oligonucleotides use for SSH	32
3.1.2.2.5. Subtraction procedure	32
3.1.2.2.6. Cloning and Sequencing	33
3.1.2.2.7. Reverse transcription and quantitative PCR (qRT-PCR) analysis	33
3.1.2.2.8. Whole mount in situ hybridization (WM-ISH)	34
3.1.2.2.9. Fixation	34

3.1.2.2.10. Decalcification	34
3.1.2.2.11. In-situ hybridization to RNA	35
3.1.2.2.11.1. Preparation of labeled RNA probes	35
3.1.2.2.12. Paraffin sectioning and photography	35
3.1.2.2.13. DAPI nuclear staining	36
3.2. <i>Amphiura filiformis</i>	36
3.2.1. Animal collection and stabling condition	36
3.2.2. Regeneration experiments on explants	36
3.2.2.1. Fixation	36
3.2.2.2. Stereomicroscopy (SM)	37
3.2.2.3. Scanning electron microscopy (SEM)	37
3.2.2.4. Light microscopy (LM)	37
3.3. <u>Other comparative models: <i>Ophioderma appressa</i> and <i>Ophioderma cinerea</i></u>	37
3.3.1. Animal collection and stabilizing conditions	37
3.3.2. Regeneration experiments in the alive models	38
3.3.3. Preliminary molecular analysis of <i>O. appressa</i>	38
3.3.3.1. DNA extraction	38
3.3.3.2. Degenerative primers design and cloning	38
4. Results and discussion	39
4.1. <i>Ophioderma longicauda</i>	39

4.1.1. Morphological analysis	39
4.1.1.1. Scanning electron microscopy (SEM)	39
4.1.2. Molecular biology	44
4.2. <i>Amphiura filiformis</i>	51
4.2.1. Microscopy	51
4.2.2.1. Stereomicroscopy (SM), Scanning electron microscopy (SEM) and Light microscopy (LM)	52
4.3. <i>Ophioderma cinerea</i> and <i>Ophioderma appressa</i>	63
4.3.1. Morphological analysis	63
4.3.1.1. Light Microscopy	63
4.3.2. Molecular biology preliminary results in <i>O. appressa</i>	67
Conclusions	68
Acknowledgments	
References	

Abstract

Regeneration processes are very complex developmental phenomena, occurring in adult and larval organisms, which require not only new cell formation but also detailed information to specify the identity of tissues to be generated at the wound site. Regeneration after injury requires several changes in terms of activation of cellular mechanisms, activities and behavior and regenerating tissues initiate diverse processes such as wound healing, programmed cell death, dedifferentiation/transdifferentiation, stem (or progenitor) cell proliferation, differentiation. Regeneration, in which lost or damage tissue are re-grown, requires specification of the identity of new tissues to be made at specific positions. In general, it is not yet understood whether this process relies only on intrinsic regulative properties of regenerating tissues or whether positional information provides input into tissue re-patterning. However, there are still few established experimental systems that enable the study of this issue in regenerating animals, especially considering animals closely related to vertebrates, the echinoderms, which are a deuterostomian, group phylogenetically related to chordates. Larval and adult echinoderms from each of the five classes present a natural and rapid regeneration potential. Among echinoderms, ophiuroids (or brittlestars) are well known for possessing a remarkable regeneration plasticity, in many species expressed by the ability to rapidly and completely regenerate arms lost following self-induced (autotomy) or traumatic amputation. In spite of the well documented regenerative phenomena, there is still a huge lack of studies providing large-scale identification of genes involved in the molecular architecture of ophiuroid wonderful regeneration capabilities. Therefore, this thesis focuses on the study of cellular and molecular aspects of arm regeneration in ophiuroid models.

As far as the cellular aspects are concerned different approaches were followed. The first one followed the overall arm regeneration process in *Ophioderma longicauda* model. Microscopic analysis allowed the characterization and reconstruction of the main phases in its morphogenetic and histogenetic events from self-induced amputation event up to 12 weeks regrowth. This results confirmed that arm regeneration in ophiuroids is achieved through a combination of morphallactic and

epimorphic processes involved both in recycling and reorganization of old tissues and blastema formation. In addition, a rough comparison with the regeneration phenomena in other close species, *Ophioderma appressa* and *Ophioderma cinerea*, was provided in order to confirm the general aspects of the process. The second approach was focussed on another model species, *Amphiura filiformis*, whose arm regeneration process has been previously studied in detail. Hence, the selected experimental model was the explant, i.e. an isolated arm fragment obtained by a double amputation of the arm, proximal and distal maintained in living conditions up to 39 days. Here the morphogenetic and histogenetic events leading to the regrowth of a regenerating arm from the distal explant end were reconstructed in order to complement the previous results of the normal arm. The explant regeneration following double amputation in *A. filiformis* demonstrated a clear developmental polarity expressed by regeneration of the arm on the distal end and by cicatrization on the proximal end.

As far as the molecular aspects, the work was addressed by trying to identify misregulated genes during early regenerative processes in arm regeneration of *O. longicauda*. An SSH library resulted in the identification of a fragment of the cDNA encoding the DNAJ, subfamily C member 7-like (*DNAJC7*) protein from regenerating arms (24 and 48 hours). This 341 bp cDNA clone matches to the 3'UTR region of a *Strongylocentrotus purpuratus* DNAJ ortholog (79% identity), a member of the DNAJ heat shock proteins (HSP 40) family. The optimized set up of *in-situ* hybridization (ISH) on the whole animal arm showed a clear expression in the radial water canal system (RWC) of both the freshly cut and the regenerating arm at 24 h and 48 h. A quantitative qRT-PCR disclosed a marked up regulation of this gene during regeneration. Based on the above-mentioned evidences we hypothesized a potential involvement of *DNAJC7 like* in arm regeneration in the ophiuroid *O. longicauda*.

Keywords: Echinoderms, ophiuroids, arm regeneration, explants, molecular aspects, misregulated genes, DNAJ

List of Tables

	Page
Table 1. Summary of the five extant echinoderm classes	12
Table 2. Gene specific primers designed for <i>O. longicauda</i> experiments	32
Table 3. Oligonucleotides use for SSH library construction	34
Table 4. Correspondence of regenerative stages between normal arm and explant of <i>A. filiformis</i>	61

List of Figures

	Page
Figure 1. Diagram of ophiuroid general anatomy	13
Figure 2. Diagram in sagittal section of ophiuroid arm anatomy following natural autotomy	14
Figure 3. Generalized scheme of ophiuroid arm regeneration	16
Figure 4. Comprehensive aboral view of the double-amputated explant	19
Figure 5. <i>O. longicauda</i> and classification	24
Figure 6. Scanning Electron Microscopy (SEM) details of <i>Ophioderma longicauda</i> arm anatomy.	25
Figure 7. <i>A. filiformis</i> classification.	26
Figure 8. <i>O. appressa</i> classification.	26
Figure 9. <i>O. cinerea</i> classification.	27
Figure 10. <i>O. longicauda</i> . SEM views of the stump and the regenerative arm (0 h – 3days).	41
Figure 11. <i>O. longicauda</i> . SEM views of the stump and the regenerative arm (1-12 weeks).	42
Figure 12. Structure of a typical sea urchin protein coding mRNA	46
Figure 13. <i>In-situ</i> detection with antisense (AS) probe of <i>OIDNAJC7</i> (A-H).	47
Figure 14. <i>In-situ</i> with sense probe of <i>OIDNAJC7</i> (A-D).	48
Figure 15. qPCR analysis of <i>OIDNAJC7</i> gene after 24 h regeneration relative to 18S.	50
Figure 16. qPCR analysis of <i>OIDNAJC7</i> gene after 48 h regeneration relative to 18S.	50
Figure 17. <i>A. filiformis</i> explants: whole mount stereomicroscopy.	57
Figure 18. <i>A. filiformis</i> explants: whole mount (SEM).	58
Figure 19. <i>A. filiformis</i> explants: Light microscopy (LM) of semi thin sagittal resin sections.	59
Figure 20. <i>A. filiformis</i> explants: Light microscopy (LM) of semi thin sagittal resin section.	60
Figure 21. <i>Ophioderma cinerea</i> : arm regeneration phases at Stereomicroscope.	65

1. Introduction

1.1. The phylum Echinodermata

1.1.1. Echinoderm bauplan and general features

Echinoderms (whose name means: *spiny skin*) are well known marine invertebrates. They are true deuterostomian coelomates derived from sessile ancestors (Hyman, 1955) and are defined by at least five main distinctive features shared by every species in the phylum. First of all, adult echinoderms are generally constructed according to evident pentameric symmetry (Hyman, 1955) visible in their external and internal anatomy. A second important character is their calcitic dermaskeleton, i.e. a true endoskeletal tissue derived from mesodermal cells, whose inorganic calcium carbonate component is organized in a peculiar porous pattern, the *stereom* (Storch *et al.*, 2005). This endoskeleton is laid down at different times in development and differently developed and located in the adults, where it can consist of a coherent, immovable shield of sutured plates as in the test of echinoids, or can be composed of numerous separated spicules or ossicles that can be joined together in movable or semi-movable articulations. The projecting spines are also extensions of the skeleton. The third character that defines the phylum echinodermata is the water-vascular system, i.e. a complex system of coelomic canals, consisting of a central circumoral ring plus five radial canals which develop in five rays according to the specific body shape (armed, globular, elongated) and gives rise to external projections, the tube feet or podia (Fig. 1a). These latter emerge from the body surface and are employed as multifunctional micro-appendices in a range of different activities (locomotion, feeding, respiration, and sensory reception, excretion) (Blake, 1990). Another important echinoderm feature is the complex tripartite structure of the nervous system: in fact it is formed by three different sub-systems placed at different levels in the body, the ectoneural system, the hyponeural and the entoneural systems (Storch *et al.*, 2005). Finally, a last intriguing distinctive feature is the presence of a peculiar connective tissue, called MCT (Mutable Collagenous Tissue), (Wilkie, 2001) capable to modulate its mechanical properties under nervous control. In spite of these common characters, echinoderms exhibit a remarkable diversity in terms of

morphology, sizes, and life style that can range from sessile or sedentary to movable life, benthonic, or even planktonic.

The phylum Echinodermata is divided into five extant classes summarized in Table 1.

Table 1. Summary of the five extant echinoderm classes. Key characteristics are adult features unless specified as larval. At least one species in each class exhibits direct development (brooding or otherwise) from a fertilized egg to the juvenile form

Echinoderm Class	Common Names	Approx. # of Living Species	Key Characteristics
Crinoidea	Sea lilies; feather stars	700	Stalked sessile echinoderms or movable stalkless forms, larvae with or without skeleton
Holothuroidea	Sea cucumbers	1200	Sluggish body, sparse microscopic skeletal spicules
Asteroidea	Sea stars (starfish)	1500	Perfect symmetry, robust skeleton, splendid colors, oblong larvae without skeleton
Echinoidea	Sea urchins; sand dollars; sea biscuits	950	Solid test with spines, Aristotle's lantern, echinopluteus larvae with skeleton
Ophiuroidea	Brittle stars; basket stars (serpent stars)	2000	Graceful, flexible, brittle arms, great phenotypic diversity, ophiopluteus larvae with skeleton

1.1.2. Ophiuroid distinctive features

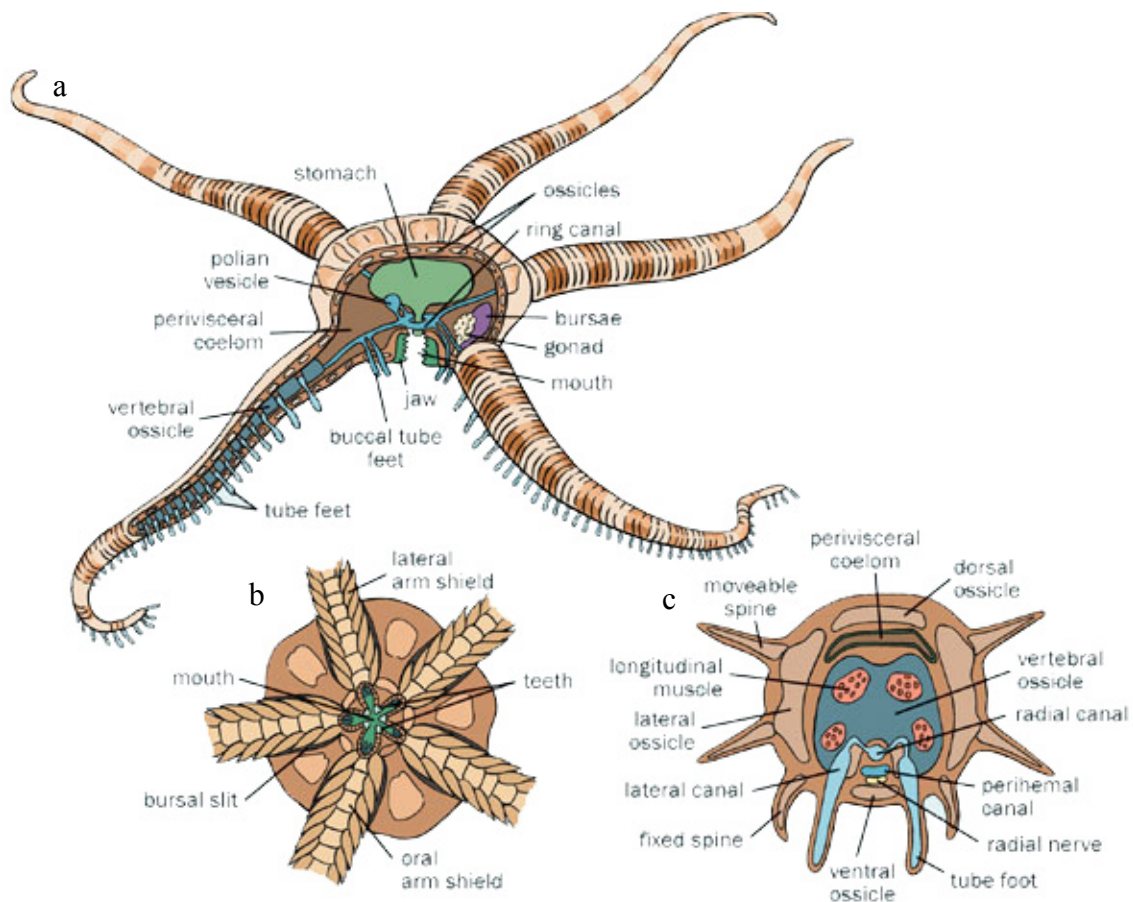


Figure 1. Diagram of ophiuroid general anatomy From Myers, P., R. Espinosa, C. S. Parr, T. Jones, G. S. Hammond, and T. A. Dewey. 2015. The Animal Diversity Web (online). Accessed at <http://animaldiversity.org>.

Within the class ophiuroidea there are the commonly known as *brittlestars* (due to the facility to break their arms) or *serpent stars* (because of the sneaky appearance of the arms (Hyman, 1955). Ophiuroids are characterized by five long sinuous arms well distinct from the roundish central disc, although, species with six, seven and up to ten arms are also known. Most species are moderate in size with disc diameters between 3 mm and 50 mm; the largest species of basket stars can have discs up to 150 mm diameter. The arms are supported by a double endoskeleton, formed by a superficial armour of protective plates provided with spines (oral shields, aboral shields, lateral shields), and a deep component of vertebral ossicles joined by movable articularions and are very flexible, exhibiting a movement reminiscent of that of snakes (in Greek *ophis* = snake). Intervertebral muscle bundles (oral muscles and aboral muscles) (Fig. 1c) and one large intervertebral ligament connect together the adjacent vertebral ossicles. Brittle stars, when stressed, easily fragment their arms by autotomy, a phenomenon due to the peculiar properties of the connective tissues, particularly those forming the

ligaments and the tendons, that display *mutability* (MCT) (Wilkie, 2001) as in many other echinoderms. Natural autotomy can occur at the level of any articulations (Fig. 2).

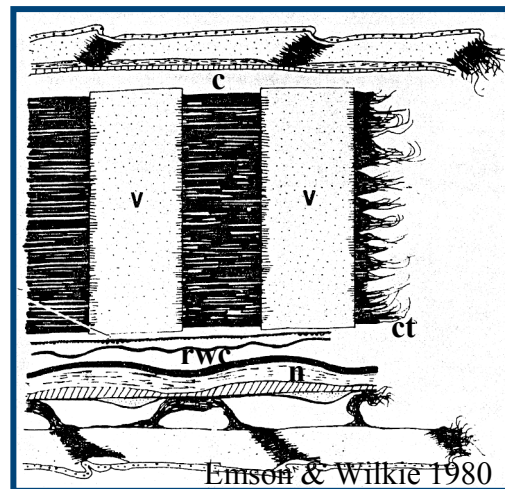


Figure 2. Diagram in sagittal section of ophiuroid arm anatomy following natural autotomy. The autotomy plane is characterized by the remains of soft tissues. In this simplified view only ligamentous connective tissues are shown; the muscles bundles are omitted. Coelom (c), vertebral ossicle (v), connective tissue (ct), radial water canal (rwc), nerve (n). From (Emson & Wilkie, 1980)

Ophiuroids have a large, star-shaped mouth centrally located on the ventral (oral) side and provided with five jaws (Fig. 1b). Digestion and absorption occur in the stomach-sac, which does not show any extension in the slender arms. Although brittle stars, as all the other echinoderms, do have the typical water-vascular system provided with tube feet, these latter are exposed externally without any protective ambulacral groove. Moreover the podia lack suckers and are rarely used for locomotion, functioning more as sensitive tactile organs or as filter-feeding tools. Instead, ophiuroids locomotion is performed by twisting and coiling the arms, pushing against the surface like a snake or gripping objects and pulling themselves forward.

The nervous system mainly consists of the ectoneural and the hyponeural components, the entoneural sub-system being very reduced. A central nerve ring (formed by only hyponeural component) runs around the esophagus and gives rise to five radial nerve cords (formed by associated ectoneural + hyponeural components), which runs into the arms until their tips. The radial nerve cords, which run along the grooved oral vertebral side, shows a typical ganglionated structure and are closely associated to peculiar coelomic components, an epineural canal, and to a hyponeural canal, running in the oral side. The haemal system (radial haemal canal) is located in the vertical

septum of the hyponeural radial canal and form branches into the podia (Hyman, 1955) (Fig. 1a). No true eyes have been found in ophiuroids, but arm plates, functioning as calcitic microlenses above light sensitive tissues have been identified in several phototactic species of the genus *Ophiocoma* (Joanna Aizenberg, 2001).

Sexes are generally separated, although some species are hermaphroditic. The gonads are located in the central disk and open into integumental slits (*bursae*) placed at the bases of the arms (Fig. 1b), which also serve as respiratory organs. Gametes are then released into the water. Several species employ the bursae to incubate developing larvae (Hyman, 1955).

1.2. Regeneration

1.2.1. Regeneration in animal biology

Regeneration is essential to the survival of all organisms. Without the ability to repair damage, organisms would succumb to the pressures associated with normal everyday existence. Regeneration, i.e. the repair and regrowth of cells, tissues, and organs to replace body parts, organs and/or appendages, after their loss or severe injury is widely but non-uniformly represented across all animal phyla, the manner and effectiveness in which repair is carried out depending on 1) the complexity of the systems; 2) the available resources; 3) the individual histogenetic and morphogenetic potential, which allows the expression of new developmental programs or re-expression of old ones at all life stages. Regeneration processes are very complex developmental phenomena, occurring in adult or larval organisms, which require not only new cell formation but also detailed information to specify the identity of tissues to be generated at the wound site. Regeneration after injury requires several changes in terms of activation of cellular mechanisms, activities and behavior (King & Newmark, 2012) and regenerating tissues initiate diverse processes such as wound healing, programmed cell death, dedifferentiation/transdifferentiation, stem (or progenitor) cell proliferation, differentiation. Regeneration generally involves the early formation of a wound epithelium after transection or injury, followed by true regenerative processes which imply both the intervention of progenitor cells involved in proliferation, migration and differentiation phenomena combined to massive morphogenesis phenomena which altogether lead to the regenerate growth (Fig 3).

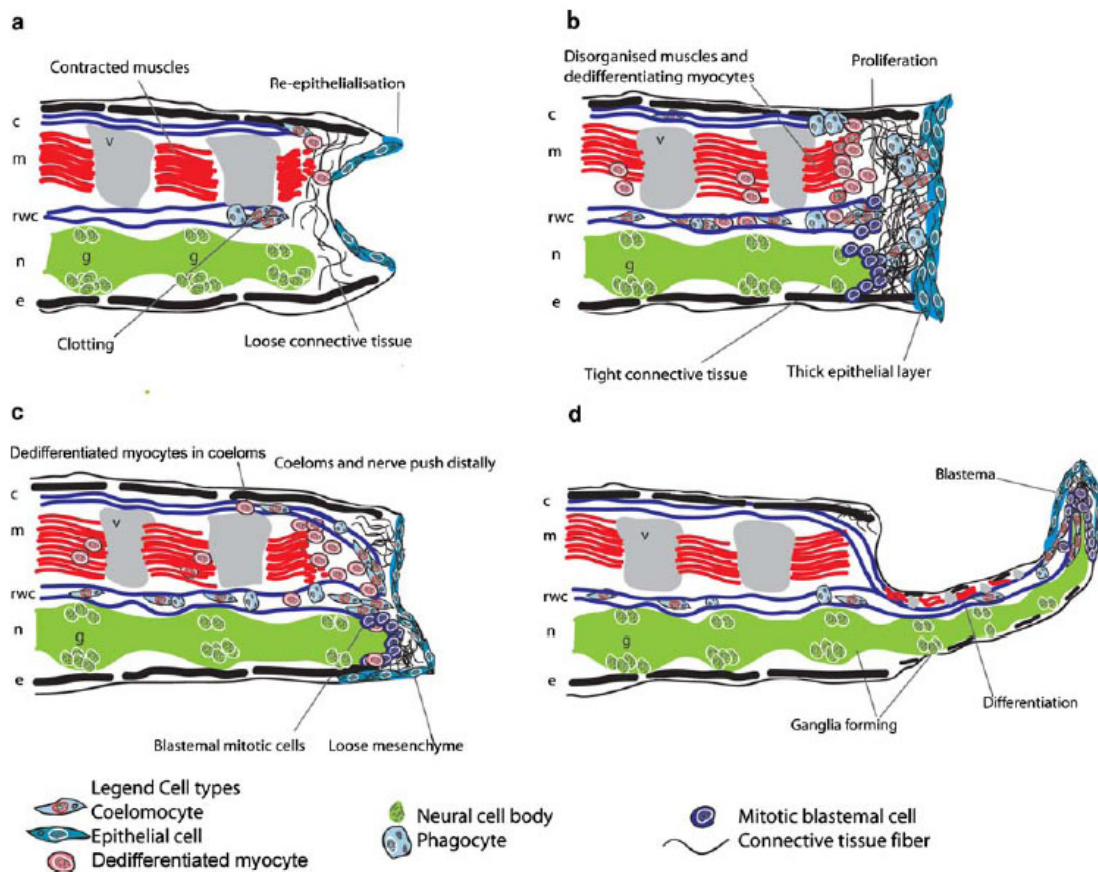


Figure 3. Schematic view of ophiroid arm regeneration (based on *A. filiformis*, emphasizing the common aspects of the overall regenerative process). **a. *Repair phase***: sealing of coelomic canals and cavities by clotting of free coelomic cells and contraction of muscles; re-epithelialization of the autotomy surface through reorganization of epidermis and contribution from migratory cells; rearrangement of tissues, nerve, connective tissues, muscles and epithelia; formation of a loose connective stroma beneath the epithelium; first signs of cell migration, proliferation and dedifferentiation begin to take place. **b. *Early regenerative phase***: complete healing of the epithelial layer; migration and proliferation of cells forming a dense mesenchyme with undifferentiated cells and phagocytes; free cells inside the coelomic cavities; the coelomic components and the radial nerve are surrounded by a few continuous layers of dividing undifferentiated cells (blastema cells) and projecting forward to define a pre-blastema area. **c. *Intermediate regenerative phase***: formation of a regenerative blastema growing orally together with the regrowing ends of the radial nerve cord and the radial water canal; multilayered epithelium ensheathing the blastema; morphogenesis and differentiation processes concentrated in the regenerative blastema; radial nerve cord reforming its ganglionated structure along with the coelomic compartments. Dedifferentiated myocytes and free coelomic cells supports with new cells. **d. *Advanced regenerative phase***: development of a miniature arm by extensive growth, morphogenesis, and differentiation processes; the proximal part acquires the distinctive internal and external features of a complete functional arm, whereas the distal portion is still undifferentiated and maintains

typical blastemal features. *m* muscles, *v* vertebrae, *n* radial nerve, *g* ganglion, *b* blastema, *rwc* radial water canal, *c* main coelomic cavity, *ct* connective tissue, *p* podia. From (Biresi et al., 2009)

These newly regenerated tissues must combine polarity and positional identity cues with preexisting body structures. We do not understand regeneration as an evolutionary variable, in particular why some animals regenerate and others apparently do not (Brookes *et al.*, 2001); (Goss-Custard, 1969); (Sanchez Alvarado, 2000). It is important then, to start understanding if this process could be an intrinsic regulative property of regenerating tissues or positional uniqueness into tissue re-patterning. On its whole, regeneration appears to present the same problems of cellular identity and positioning characterizing the embryonic development: however, in regeneration, the genetic program that determines particular cell fates is not irreversibly established (Davidson *et al.*, 1998) a major difference being the tissue context in which the process takes place. In fact, during regeneration, the new cell developed in an already established location of adult tissues. Furthermore, it is important to characterize the program or re-expression processes that occur during this post-embryonic development.

Echinoderms are well known for their striking regenerative capabilities. Regeneration is perhaps one of the most familiar aspects of echinoderm biology. For this reason and due to their phylogenetic position closely related to chordates (Ferraz Franco *et al.*, 2014) they offer excellent example of complex and highly evolved organisms on which regeneration studies should be extensively addressed. It is probable, in fact, that mechanisms controlling echinoderms regeneration may operate also in chordates, including vertebrates. As a result, echinoderms have the potential to offer a variety of viable and *tractable models* for a comparative holistic approach to regeneration including molecular, cellular and tissue aspects (Candia Carnevali. & Bonasoro, 2001). Echinoderms with their amazing capability for regeneration have even the potential to exploit regeneration in a part detached from the body. As an example, *explants* (arm segments isolated from the animal body) (Fig. 4), when detached from the *donor* animal still display a great regenerative potential in several groups (crinoids, asteroids, ophiuroids) (Candia Carnevali *et al.*, 1998). Even the amputated arm segments (*explants*), once isolated from their donor arms and re-amputated in

their distal end, cannot only survive in good living conditions for several weeks and repair the wounds, but even undergo extensive regenerative processes in its distal end. Moreover, when subjected to a second distal amputation, these double-amputated explants can even undergo extensive regeneration of their distal tips which is not limited to early blastemal stages but progresses until advanced stages, whereas their proximal ends continue to show simple healing without subsequent regrowth, indicating a programmed developmental polarity within the arm (King & Newmark, 2012). The ophiuroid arm explant can therefore represent a simplified and controlled regenerating *in vivo* system, providing a valuable test of assumptions in terms of mechanisms and processes.

1.2.2. The explants and double explants

Since arm explants (Fig. 4) have shown a remarkable capacity of survival and long-term autonomy (Candia Carnevali *et al.*, 1998) they could be a very useful, simple and basic model to investigate elementary influences of the local tissue on regeneration. In spite of this attractive perspective, the experimental employment of arm explants in the study of regeneration, previously successfully applied only in the crinoid models (Candia Carnevali *et al.*, 1998), was never attempted in ophiuroids. Because of the striking and unexplored regenerative potential described above, *A. filiformis* is therefore an ideal candidate to study in parallel, and in the same individual, arm and explant regeneration comparing the two models and underpinning similarities and differences in the two processes. The morphogenetic and histogenetic potential of these regenerative models is spectacular. In both arm or explants regeneration, the amputated stump can simply undergo modest repair processes or very complex regenerative processes, not by resorting to a direct regrowth of specific cell / tissue types, but employing a few types of progenitor cells (undifferentiated or dedifferentiated) which, through migration, proliferation and differentiation processes associated to appropriate morphogenetic mechanisms, can restore the original morphology of the entire arm in its functional integrity (Fig. 1,2,3, for reviews, see (Hernroth *et al.*, 2010) and references therein) by closely maintaining a directional growth and polarity.

Indeed the explants must be certainly considered good and unique tools for studying peculiar aspects of the regenerative phenomena: for instance, the ability of the double-amputated explants to successfully survive independently from their donor animal for many weeks; the capability to undergo autonomous regeneration processes quite comparable to those described in normal regenerating arms (Biressi *et al.*, 2009); finally the evident different regenerative cues displayed respectively by the explant proximal and distal ends, which are indeed offering the perfect experimental conditions for exploring the aspect related to programmed polarity during regeneration. Polarity during regeneration is a complex mechanism, driven by intra- and intercellular forces, and genetic processes, regulated by an array of signaling molecules (King & Newmark, 2012; Yokoyama, 2008). In *A. filiformis*, the factors controlling regeneration and polarity of response must already be present or be produced within the amputated arm, although at present nothing is yet known.

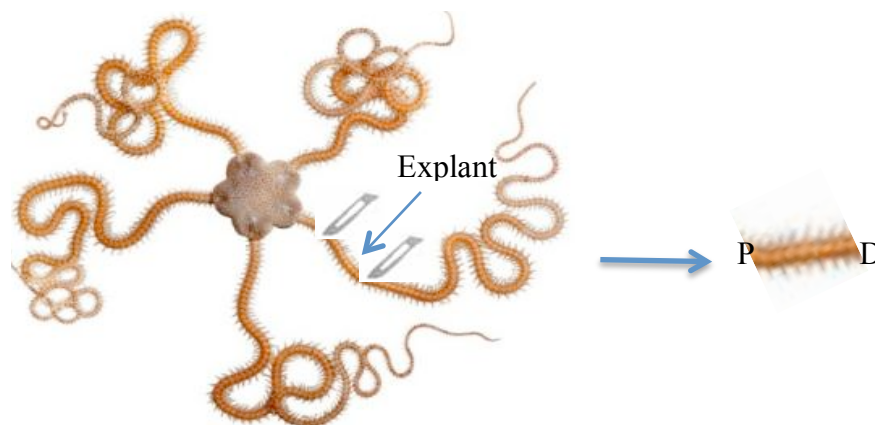


Figure 4. Schematic view of the double-amputated explant and its donor animal. double-amputated explant length: 1 cm. **P.** Proximal amputation; **D.** Distal amputation.

1.2.3. Regenerative mechanisms and model systems

Humans are fascinated with the capacity to regenerate body parts, since we are so poor at it ourselves. Even so, some mammalian structures do regenerate: mammals regenerate various tissues including peripheral nerves, bones, skeletal muscles, liver tissue, and blood vessels (Carlson, 2005); however, they lack the ability to regenerate key structures such as organs (with the notable exception of the liver).

In spite of the obvious relevance of the regeneration processes for both basic and applied biology, and in spite of an old tradition of historical studies on animal

regeneration, modern comprehensive studies addressed to investigate the overall regenerative phenomenon are not so numerous as expected and the models explored so far are only a few, the most extensively studied among invertebrates being the freshwater hydra (Gierer *et al.*, 1972), planarians (Sánchez Alvarado, 2004), leeches (Tettamanti *et al.*, 2005), squids (Detrait *et al.*, 2000), insects (Galko & Krasnow, 2004) and echinoderms (Candia Carnevali, 2006).

Although in the last decades regeneration has been well explored also in a number of vertebrate models including fish (Reimschuessel, 2001), frogs (Bement *et al.*, 1999), newts (Donaldson *et al.*, 1985), mice (Seifert *et al.*, 2012), rabbits (Angius *et al.*, 2012), pigs (Atkinson *et al.*, 2014) and of course humans (Elangovan *et al.*, 2013; Lin *et al.*, 2014), new models are indeed needed to fully understand this process, with particular reference to organisms belonging to animal groups closely related to vertebrates.

As stated above, echinoderms are good models to study, not only because of their phylogenetic position close to vertebrates (sea urchin genome shares approximately 70% of the genes with the human genome) (Sea Urchin Genome Sequencing *et al.*, 2006), but also for their experimental tractability, in terms of availability and adaptability of *in vivo* models. Larval and adult echinoderms from each of the five classes present a natural, rapid and vast regeneration potential: in particular the ability to regenerate appear to be related to the widespread self-mutilation phenomena, employed as a defense response (autotomy) to predators attack, unfavourable environmental conditions, or seasonal changes. Following autotomy a number of structures can be rapidly and effectively regenerated: different body parts, arms, external appendages (spines or tube feet) (Dubois & Ameye, 2001), entire organs, visceral mass (following evisceration) (Garcia-Ararras *et al.*, 1999). At the same time, regeneration has developed as a true part of a program of asexual reproduction where *fission* processes result in two or more new individuals (Candia Carnevali, *et al.*, 2001). For instance, many asteroid species can usually form entirely new individuals when bisected (Speman, 1938), and a few species (*Linckia* sp., *Coscinasterias* sp.) can even regenerate a whole animal from an isolated arm (Cuénot, 1948). Indeed, the importance of these phenomena for the phylum was recognized at

an early date by Rüggenbach (1903) who wrote “*in no group of animals is self-mutilation so generally widespread as in the echinoderms.*”

These results clearly indicate a strong plasticity and great potential in echinoderms and suggest employing these models for investigating correlation across echinoderm and vertebrate species on the different biological aspects. Due to the remarkable regenerative capabilities and vicinity with vertebrates, echinoderms present promising perspectives in the applied field of regenerative medicine when compared to other deuterostomians, which are more likely to be extended to mammals than those observed in other classical models such as hydra or planarians, which are much more distant from chordates. Also, echinoderms offer a wide range of experimental models more tractable and not subjected to any ethic restrictions in respect to other animal models widely used in the experimental approach, such as zebrafish and amphibians. Furthermore, the ability of a deuterostomian animal to regenerate a lost limb is an area of particular interest to researchers trying to unlock the key to regeneration in mammals because regeneration can represent a true cure of a disease state (Brockes & Kumar, 2005; Stocum, 2002).

1.2.4. Regeneration at cellular and tissue level

Regeneration is in fact a post-embryonic developmental process. It involves recruitment of stem cells and/or dedifferentiated cells, cell proliferation and migration, provision of specific regulatory factors and finally expression and re-expression of the developmental program in adult animals. Capabilities seem to depend upon individual potential in terms of expression, or re-expression of specific developmental program, and of histogenetic and morphogenetic plasticity (Wadman, 2005; Weissman, 2000; Candia Carnevali, 2006). In terms of general mechanisms, regeneration in all animals involves one or two basic process, epimorphosis, and morphallaxis. In epimorphosis, new tissues are formed from undifferentiated cells, stem cells or dedifferentiated cells forming a blastema, which is a distinct local center of intensive cell proliferation and growth. Instead, morphallaxis implies less extensive and localized proliferation of cells that are derived from existing tissues by dedifferentiation, transdifferentiation, and/or migration, and results in a direct regrowth of the stump tissues. Epimorphosis and morphallaxis mechanisms are both

present in echinoderms. Epimorphosis with a blastema formation seems to be typical when regeneration is a predicted, rapid, and effective phenomenon, which takes place following autotomy (Candia Carnevali *et al.*, 1998; M. Candia Carnevali *et al.*, 2001). These epimorphic mechanisms seem to reutilize mostly embryonic developmental processes and on their whole follow pre-established phases. On the other hand, morphallaxis appears to be a phenomenon more frequent after traumatic mutilation, where amputation is not predictable and subsequent regeneration process are slower and more complicated (Thorndyke & Candia Carnevali, 2001). This mechanism significantly infers in the rearrangement of the old structures, appearing to be unique to regeneration and not shared by embryonic development.

1.2.5. Regeneration in Ophiuroids

Among echinoderms, brittlestars are well known for possessing a remarkable regeneration plasticity expressed in the different groups, at both larval and adult stages, with a significant degree of diversity. In many species, adult individuals possess the ability to undergo complete arm regeneration with arm repair rates in excess of 90% of individuals sampled depending on the population (Burns *et al.*, 2011; Kurdziel, 1994; Lawrence, 2010). Fission and regenerative phenomena are well known and described in both adults and larvae, and are also remarkably well documented in fossils of extinct brittlestar species (Aronson, 1987, 1992). In ophiuroids, arm regeneration is the most explored phenomenon. They often cast off arms at all levels, with breakage occurring at an autotomy plane after damage, attack, or handling. Ophiuroid echinoderms can lose arms due to traumatic amputations or can undergo autotomy as a self defense mechanism (Wilkie, 2001): in all cases they completely regenerate the lost arms. In addition, even the amputated arm segments (explants), once isolated from their donor arms and reamputated in their distal end, can not only survive in good living conditions for several weeks and repair the wounds, but even undergo extensive regenerative processes in its distal end. The ophiuroid arm explant can therefore represent a simplified and controlled regenerating *in vivo* system, providing a valuable test of assumptions in terms of mechanisms and processes. In both regenerating arm and explant, immediately following autotomy, epidermal cells expand, migrate, and spread over the wound and blastema forms from accumulated coelomocytes (Candia Carnevali, 2005; Biressi *et al.*, 2009). Evidence suggests that a

combination of morphallaxis and epimorphosis is responsible for regeneration in ophiuroids. In fact morphallactic mechanisms, as can be considered those comprising expansion and migration of epidermal cells as part of the initial wound-healing process, are followed by local accumulation of coelomocytes that proliferate resulting in the rapid formation of an epimorphic blastema-like structure (Thorndyke *et al.*, 2000).

Despite this background in ophiuroids, cellular and molecular aspects of the regeneration process are little understood and most of the work available has been focused on the ecological benefits and impacts of the extensive regeneration seen in many species (Stancyk *et al.*, 1994). To date, molecular events surrounding regeneration in echinoderms have been poorly characterized. However, in recent years, studies have shown that echinoderms have the potential to offer viable and tractable models for exploring in detail molecular and cellular aspects of regeneration (Bannister *et al.*, 2008; Ben Khadra *et al.*, 2014; Brockes & Kumar, 2008; Burns *et al.*, 2011; Burton & Finnerty, 2009; Patruno *et al.*, 2003), giving space to an ample field of questions to be answered.

1.3. The experimental models

1.3.1. *Ophioderma longicauda*: general features

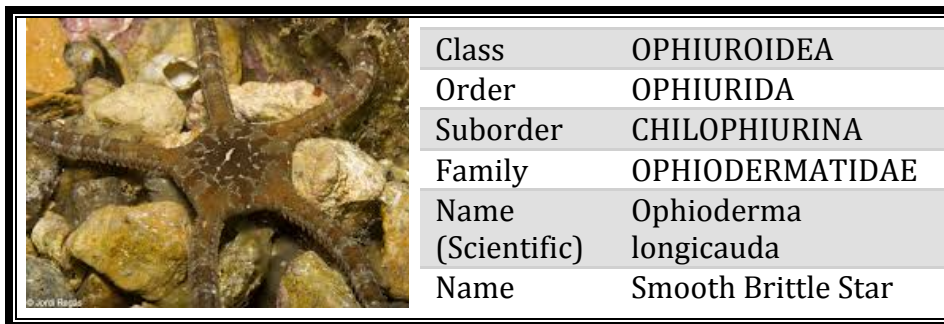


Figure 5. *O. longicauda* classification.

It is found from surface to 70 m deep mainly in rocky bottoms in the Mediterranean Sea and in the Atlantic up to the Western Brittany coasts where it is rather rare. Its surface is smooth with a fine granulation and a leathery texture with a pentagonal disc of about 3 cm across. On the ventral side between the arm bases there are five pairs of grooves. The five very slender arms each can reach 15cm length. The color of this species is usually chocolate brown but may also be red-orange, dark brown or black (Fig. 5) The arms often have lighter, greenish bands. The ventral side with the mouth, containing a five-toothed jaw, is paler. *O. longicauda* is photophobic and therefore hides below rocks by day. By night it feeds very actively and voraciously on worms and bivalves buried in the sediment but also carrion and detritus. It is an efficient predator and can scent its prey on greater distance. Lost arms are regenerated quickly. Brittle stars usually mature at the age of 2 years and can live up to 5 years.

1.3.1.1. *Ophioderma longicauda*: arm anatomy

Ophiuroids arms are joined by movable articulations covered by four superficial skeletal plates: one aboral, one oral, and two lateral arm shields with spines (Fig. 6b, c, k). The complex of the shields form a complete superficial endoskeletal armour along with a longitudinal series of vertebral ossicles, these latter forming the inner solid core of the arm (Fig. 6h). Muscles and ligaments connect vertebral ossicles to each other by two pairs of intervertebral muscles, namely two oral and two aboral muscles, and one large intervertebral ligament (Fig. 6d, e, h, i, j). The radial nerve

cord runs along the oral vertebral groove, it shows a typical “ganglionated” structure and is associated to an oral epineural canal and to an aboral hyponeural canal (Fig. 6d, h). The radial water canal is located above the nerve cord (Fig. 6d, f, h) (Hyman, 1955). A pair of podia originates from the radial water canal at the level of each vertebral ossicle (Fig. 6f, g). Finally the radial haemal canal is located in the vertical septum of the hyponeural radial canal and branches into the podia (Fig. 6f).

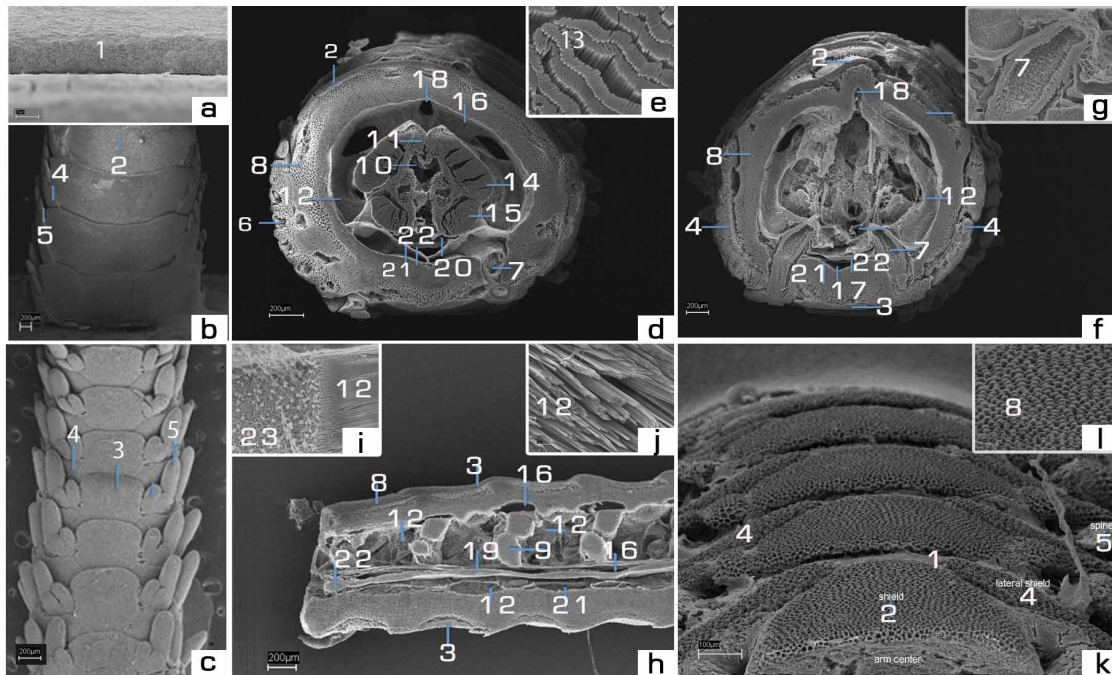


Figure 6. SEM details of *Ophioderma longicauda* arm anatomy. Section samples (d, e, f, g, h, i, j); whole samples (a, b, c, k, i). **a:** Detail of the edge of an aboral arm shield. The skeletal structure, covered by the external epithelium, looks rather compact and defined. **b:** Top view of the aboral side of the arm. **c:** Top view of the oral side of the arm. **d:** Transverse section of the arm at the intervertebral articular level. The four muscle bundles are visible. **e:** Enlargement of fig. d showing a detail of a muscle bundle. **f:** Transverse section of the arm showing the arrangement of the water vascular system, including the central radial canal and the emerging tube feet. **g:** Enlargement of the tube foot of fig. f showing its wall and internal lumen. **h:** Comprehensive view of arm microscopic anatomy in sagittal section. **i:** Enlargement of fig. h showing details of vertebral ossicle and intervertebral ligament. **j:** Detail of the intervertebral ligament. **k:** Top view of aboral shields showing the strom structure. **l:** Detail of fig. k showing the typical superficial stereom pattern. 1) Edge of aboral arm shield, 2) aboral arm shield, 3) oral arm shield, 4) lateral arm shield, 5) spines, 6) lateral spine cavity, 7) tube foot, 8) stereom, 9) oral portion of vertebral ossicle, 10) joint socket, 11) aboral portion of vertebral ossicle, 12) intervertebral ligament, 13) detailed of muscle bundles, 14) aboral intervertebral muscle, 15) oral intervertebral muscle, 16) epineural canal, 17) hyponeural canal, 18) perivisceral coelomic cavity, 19) radial nerve cord, 20) water radial canal, 21) coelomic lining, 22) nerve “ganglion”.

1.3.2. *Amphiura filiformis*: general features

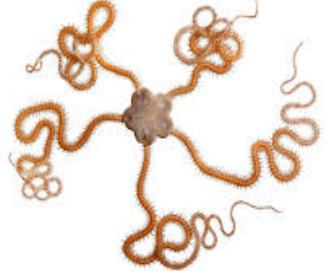
	Class	OPHIUROIDEA
	Order	OPHIURIDA
	Suborder	OPHIURINA
	Family	AMPHIURIDAE
	Scientific Name	<i>Amphiura filiformis</i>
	Name	Brittle Star

Figure 7. *A. filiformis* classification.

Its distribution varies from 5 to more than 200 m depth, in muddy sand or mud, all round the British Isles, except, possibly, the southeast. *A. filiformis* burrows about 5 cm into the substrate. The species is able to burrow down into the sediment keeping its serpentine arms sticking out from the sediment surface (Gage, 1990). The long, fine arms are about ten times longer than the diameter of the disk. *A. filiformis* is a suspension feeder, collecting mixed micro-plankton, resuspended bottom material and detritus. The arms of this brittle star have three main functions: ventilation and respiration, transport of sediment and waste materials out of the burrow, and collection and transport of food (Ockelmann & Muus, 1978). The disk of *A. filiformis* is covered with scales on the dorsal side only, leaving the ventral side naked. The diameter of disk can be up to 8-10 mm. Its colour is reddish- or greyish-brown (Fig. 7) (Hayward & Ryland, 1990).

1.3.3. *Ophioderma appressa*: general features

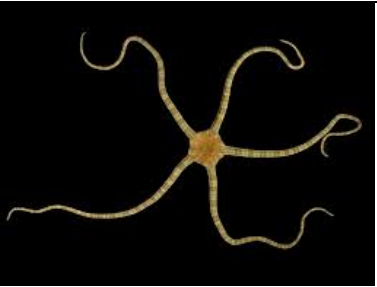
	Class	OPHIUROIDEA
	Order	OPHIURIDA
	Suborder	OPHIURINA
	Family	OPHIODERMATIDAE
	Scientific Name	<i>Ophioderma appressa</i>
	Name	Banded-arm brittlestar

Figure 8. *O. appressa* classification.

This species is common all over the Caribbean and lives under rocks, old coral heads and in recesses. It can be found on reefs and reef flats at depth from 3 m down to 20 m. It has long slender arms with a distinct central disc, circular or pentagonal, with a

diameter ranging from 4.18 to 7.89 mm, covered by small granules. The color of the disc is variable, ranging from gray or brown to white, often with spots, but may be uniform (Fig. 8). The color of the arms is gray with light bands. The radial shields are oval and covered with granules; the oral and aboral shields are broadened laterally and not covered by granules. Four short bursal slits open on the oral side. The arms are covered with scales rather than spines (Say, 1825).

1.3.4. *Ophioderma cinerea*: general features

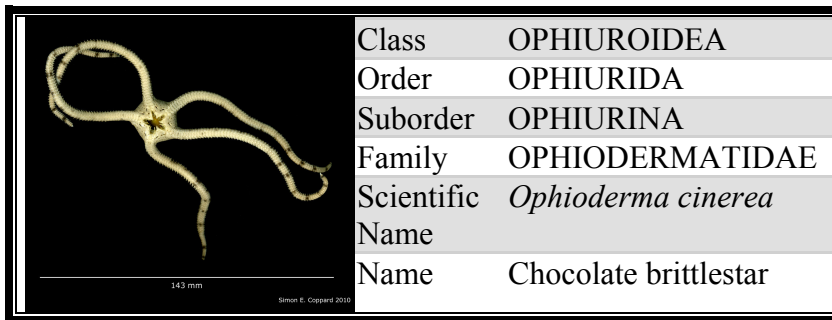


Figure 9. *O. cinerea* classification.

It is a tropical species distributed in Western central Atlantic. It is an intertidal species found in coral reefs, sea grass beds, and rubble at depth range 0 - 24 m. The disk is circular or pentagonal (4.96 to 9.67 mm) and covered by small granules, except on radial shields (Fig. 9). Radial shields are oval and oral shields heart-shaped. Aboral shields are small, laterally broadened, not covered by granules. Seven to nine small and compressed arm spines are present (Muller & Troschel, 1842).

2. Objectives

General Objective

To study cellular and molecular aspects during arm regeneration in different brittle stars thru early time points

Specific Objectives

1. To better characterize morphological internal and external structures in the arm of *O. longicauda* as regenerative model at early time points
2. To identify genes in *O. longicauda* possibly implied in regeneration at early time points
3. To better understand polarity at different morphological stages in arm explants of *A. filiformis* as a regenerative model during early time points
4. To confirm the regenerative phases of arm regeneration in Caribbean Ophiuroids

3. Materials and methods

3.1. *Ophioderma longicauda*

3.1.1. *Animal collection and stabling conditions*

O. longicauda specimens were collected by scuba divers in the Tyrrhenian coast of Italy (Giglio Island, Tuscan Archipelago and Monte Argentario, Grosseto) at a depth of 30-50 meters. Once animals were transported to Milan they were kept at 16 °C in aquaria containing coralline sand and rocks from the sampling site and supplied with artificial seawater internal circulating system. The aquaria were exposed to a 12 hours/day light cycle. Water parameters like temperature, density, nitrites, nitrates and pH were checked once a week to guarantee optimal stabling conditions throughout the experiments. Animals were fed once a week with chopped frozen cuttlefish.

3.1.2. *Regeneration experiments*

3.1.2.1. *Morphological and histological analysis*

Samples were taken from *O. longicauda* specimens that did not show any evidence of recent regeneration events mimicking the conditions of autotomy mutilations; by self-induced amputation chemically, dripping a saturated NaCl solution on the arm to be amputated. Experimental amputations were performed either at the tip of the arm or at the middle of the arm. Following the amputation, animals were left to regenerate in the aquarium for prefixed periods up to 12 weeks, for morphological analysis using scanning electron microscopy (SEM) obtaining the distal end every time point used (0, 1, 3 days and 1, 3, 6 and 12 weeks (p.a))

3.1.2.1.1. *Scanning electron microscopy (SEM) in whole arms*

After each established collection stage, a comprehensive morphological analysis of the different regenerative stages for an overall period of 12 weeks post-amputation (p.a) arm was performed in *O. longicauda*. Arm samples were fixed with 2% Glutaraldehyde in 85% seawater (SW) for 2 h at 4°C. Samples were then placed in filtered seawater (FSW) overnight at 4°C. Next day, samples were rinsed 2x with DI

water followed by a graded standard dehydration process, starting at 25% EtOH till reaching absolute EtOH. Samples were then left to dry on filter paper, mounted on stubs, covered with a thin layer of pure gold (Sputter Coater Nanotech) and observed with a LEO-1430 scanning electron microscope.

3.1.2.1.2. SEM in sectioned samples

Arm samples were fixed with 2% Glutaraldehyde in 85% SW for 2 h at 4°C. Samples were then placed in FSW overnight at 4°C. Next day samples were rinsed 2x with DI water followed by a graded standard dehydration process, starting at 25% EtOH till reaching absolute EtOH then following the standard methods for paraffin wax embedding. Embedded samples were cut with Reichert OmE till prefixed specific levels. The sectional samples were washed several times with xylene for five days till paraffin removal. After dewaxing, samples were rinsed with absolute EtOH, subsequently with different concentrations of HMDS (Hexamethyldisilazane) and absolute EtOH (1:3, 1:1, 3:1,100% HMDS). Samples were then prepared for SEM, observations as mentioned before.

3.1.2.2. Molecular biology experiments

Samples were taken from *O. longicauda* specimens that did not show any evidence of recent regeneration events; two arms were cut (with scalpel) per animal and left to regenerate up to the established time point (24 h, 48 h). Per animal, experimental amputations were performed either at the tip of the arm or at the middle of the arm. Following the amputation, animals were left to regenerate in the aquarium for prefixed periods (24 h and 48 h), for molecular analysis and ISH. Once completed the regeneration period, five segments of the amputated stump (including the regenerating part), were cut with a scalpel.

3.1.2.2.1. RNA extraction

Total RNA was extracted from control (C6B) and 24 h (6B) regenerating arm of *O. longicauda* using RiboPure™ kit, (Life technologies) following the manufacturer's instructions. RNA quality was assessed by denaturing agarose gel electrophoresis;

RNA concentration and purity were determined measuring the absorbance at 260 and 280 nm using a Spectrophotometer Bio-Rad SmartSpec 3000 UV/Vis.

3.1.2.2.2. *Suppressive Subtraction Hybridization (SSH) library (Performed by Evrogen Lab)*

SSH is based primarily on a suppression polymerase chain reaction (PCR) technique combining normalization and subtraction in a single procedure. In the normalization step occurs stabilization in the abundance of DNA fragments within the target population, and in the subtraction step occurs the exclusion of the sequences that are common to the populations being compared. These steps increase the probability of obtaining low-abundance differentially expressed cDNAs fragments and it simplifies analysis of the subtracted library without having to compare repetitive and overabundant results (Zhu *et al.*, 2001). Two libraries were generated, the regenerative (6B) library and the non regenerative (C6B) library. cDNA subtraction was performed using SSH method in both directions (6B vs. C6B and C6B vs 6B) as previously described (Diachenko *et al.*, 1996; Diatchenko *et al.*, 1999) to specifically identify the differentially expressed genes.

3.1.2.2.3. *cDNA synthesis and Rsa I digestion*

Amplified double strand cDNA was prepared from 6B and C6B RNAs using a SMART approach (Zhu *et al.*, 2001).

SMART Oligo IIA oligonucleotide and SMART CDS primer IIA were used for first-strand cDNA synthesis. For both samples, first-strand cDNA synthesis was started from 0,5 ug RNA in total reaction volume 10 ul. 1 ul of 5 times diluted first-strand cDNA was then used for PCR amplification with SMART PCR primer II A. 20 PCR cycles were performed. Each cycle included 95°C for 15 s; 65.5°C for 20 s; 72°C for 3 min.

SMART-amplified cDNA samples were further digested by *Rsa* I endonuclease.

3.1.2.2.4. Oligonucleotides use for SSH

Table 2. Oligonucleotides use for SSH library construction

SMART OligoII A oligonucleotide	5'-AAGCAGTGGTATCAACGCAGAGTACGCrGrGrG-3'
SMART CDS primer II A	5'-AAGCAGTGGTATCAACGCAGAGTA-d(T)30-3'
SMART PCR primer II A	5'-AAGCAGTGGTATCAACGCAGAGT-3'
Adapter 1	5'-CTAATACGACTCACTATAGGGCTCGAGCGGC CGCCCGGGCAGGT-3' 3'-GGCCCGTCCA-5'
PCR primer 1	5'-CTAATACGACTCACTATAGGGC-3'
Nested primer 1	5'-TCGAGCGGCCCGCCCGGGCAGGT-3'
Adapter 2R	5'-CTAATACGACTCACTATAGGGCAGCGTGGTTCG CGCCCGAGGT-3' 3'-GCCGGCTCCA-5'
Nested primer 2R	5'-AGCGTGGTCGCGGCCGAGGT-3'

3.1.2.2.5. Subtraction procedure

Subtractive hybridization was performed using SSH method in both directions (6B vs. C6B and C6B vs. 6B) as described in (Diachenko *et al.*, 1996; Diatchenko *et al.*, 1999). Briefly, the following procedures were performed:

For each direction, two tester populations were created by ligating of different suppression adapters (Adapters 1 and 2R). These tester populations were mixed with 30X driver excess (driver cDNA had no adaptors) in two separate tubes, heat-denatured, and allowed to renature. After first hybridization, these two samples were mixed and hybridized together. Subtracted cDNA was then amplified by primary and secondary PCR.

Primary PCR: 27 PCR cycles with PCR primer 1 were performed for subtracted 6B cDNA and 27 cycles - for subtracted C6B cDNA.

Secondary (nested) PCR: 10 PCR cycles with Nested primers 1 and 2R were performed for both subtracted cDNA samples.

3.1.2.2.6. Cloning and sequencing

For cloning purposes, the whole subtraction library has been amplified using the 2 universal primers **SP6**: 5'-TAC GAT TTA GGT GAC ACT ATA G-3' and **T7**: 5'-TAA TAC GAC TCA CTA TAG GG-3' flanking all the cDNAs in the library at the following conditions: 95°C for 15 s, 50°C for 20 s, 72°C for 3 min. for a total of 35 cycles.

2.0 µl of the reaction have been cloned employing TOPO TA cloning® kit (Invitrogen™) according to the manufacturer's instructions. Ten colonies were picked and growth overnight at 37°C in LB broth with ampicillin. An aliquot of the bacteria grown was stored in glycerol at -80°C; the remaining volume was used to isolate the plasmid with the PureYield™ Plasmid Miniprep System (Qiagen). Presence of DNA Plasmid was confirmed by 1% agarose gel electrophoresis. Insert positivity was confirmed by DNA restriction with *EcoRI* (two restriction sites are present on both sides of the insert). DNA automated sequencing of six clones was performed, and their similarity to genes from other species has been highlighted by the alignment with the NCBI-sequence databases using BLASTN software (<http://blast.ncbi.nlm.nih.gov/Blast.cgi>).

The sequences of the singled-out clones have been used to design gene-specific primers (Table 3) employing the Primer 3 Software (http://biotools.umassmed.edu/bioapps/primer3_www.cgi), followed by manual adjustments. 18S primers have been designed based on the most conserved regions among 18S genes from several species (insects to Vertebrates).

3.1.2.2.7. Reverse transcription and quantitative PCR (qRT-PCR) analysis

Each total RNA sample previously purified (see above) was incubated with DNaseI to eliminate any genomic DNA residue from the RNA preparation. First-strand cDNAs were synthesized employing the ImProm-II™ Reverse Transcription System (Promega, Madison, WI, USA), according to the manufacturer's protocol, using random oligonucleotides to prime the reverse transcription of 1 µg of total RNA. PCRs were performed using gene-specific primers. For normalisation purposes, 18S ribosomal RNA level was tested in all the samples analysed via quantitative RT-PCR. Reactions were performed in a 48-well format Eco Real-Time PCR System using

GoTaq qPCR Master Mix (Promega, Madison, WI, USA). Three independent qPCR experiments from the same reverse transcription sample were performed using each pair of gene-specific primers (Table 3). The presence of a single PCR product was verified by the melting-curve and the agarose gel analyses.

Table 3. Gene-specific primers designed for qRT-PCR

18s Frw:	5'- GTCCCTGCCCTTTGTACACA - 3'
18s Rvs:	5'- ACCTACGGAAACCTTGTTACGA - 3'
CO3 Frw:	5'- AGGAAGCGTGTGTTTAGCTG - 3'
CO3 Rvs:	5'- AGTCACCAAAACAGCAGTGC - 3'
GO3 Frw:	5'- TGTCCTGTAGTGAGCCAATCA - 3'
GO3 Rvs:	5'- TGCATTTTCAGTTTTGCAGTTG - 3'
FO3 Frw:	5'- TGCCCGCTGAAAAGCTTAAC - 3'
FO3 Rvs:	5'- TCCTGACCACTCTATTCGAACG - 3'
DO3 Frw:	5'- TCTGTGTTGAACGGTTAGGC - 3'
DO3 Rvs:	5'- TCCCGCCAAACTGTAAATCG - 3'

3.1.2.2.8. *Whole mount in situ hybridization (WM-ISH)*

Since ISH has never been performed in our model system, WM-ISH was specifically adapted for *O. longicauda*, making this a novel approach for this type of organisms. The thickness and tissue density of the arm made this approach very challenging and after several trials it was noticed that decalcification was key for probe penetration.

3.1.2.2.9. *Fixation*

Arm samples were fixed in 4% paraformaldehyde (PFA) in phosphate buffered saline (PBS) overnight at 4°C. Fixed material was then washed twice in PBT (PBS containing 0.1% (v/v) Tween 20 (Sigma)) for 2 min then dehydrated through 50% ethanol/PBT (10 minutes) to 100% ethanol. Tissue can be stored in 100% ethanol at -20°C for up to 1 year.

3.1.2.2.10. *Decalcification*

Several decalcification methods such as 10% sodium citrate, 20% formic acid, Morse's solution (10% sodium citrate plus 20% formic acid), 10% EDTA (pH 7.4) and 10% EDTA/TRIS-HCl (pH 7.4) were tested (Alers *et al.*, 1998) with similar

results. Morse's was preferred due to the short time incubation requested (1 day), effectiveness (good decalcification result), and preservation of mRNA.

3.1.2.2.11. *In-situ hybridization to RNA*

3.1.2.2.11.1. *Preparation of labeled RNA probes*

- a) Probes were transcribed using the PCR amplicons obtained from the amplification of each plasmid singled-out by the SSH library screening. Briefly, PCR was performed on plasmid templates using SP6 and T7 primers. Amplified DNA was purified, resuspended in RNase free water, then *in-vitro* transcribed with SP6 and T7 to obtain antisense and sense riboprobes (depending on the orientation of the insert inside the plasmid) labeled with modified nucleotides (digoxigenin, Roche). The probes were quantified using the Spectrophotometer Bio-Rad SmartSpec 3000 UV/Vis and used for the WM-ISH.
- b) Permeabilization of tissue and hybridization of the probe to the tissue: after rehydration of tissue, permeabilization was achieved by several washes with PBT (Phosphate-buffered Saline (PBS) with 10% Tween 20). Hybridization (HB) mix was prepared with 0.5 ng/ μ L of the probe. The HB mix was heated at 65 °C for 10 min, cool on ice for 10 min then heat up to 45°C. Mix was then incubated overnight (ON) at 45°C.
- c) Washing to remove unhybridized probe: Removal of unhybridized probe was done with several washes at different concentrations of hybridization buffer (HB) and PBT.
- d) Signal detection: Detection of the probe was performed by incubating the arms with blocking buffer (BB - PBT plus sheep serum) for 2 h, then adding 0.1 μ l of antibody Anti-Digoxigenin-AP, Fab fragments (Roche), finally incubating the samples ON at 4°C. Over stained samples were washed with AP buffer (1M Tris pH 9.5, 5M NaCl, 1M MgCl₂, 10% Tween 20, 1M levimasole). Signal detection reaction was stopped with PBT buffer.

3.1.2.2.12. *Paraffin sectioning and photography*

After WH-ISH protocol, the samples were dehydrated in an ethanol series and then embedded in paraffin wax according to standard methods. Stained sections were cut

with a Reichert OmE at 8µm and, after dewaxing and rehydration, they were permanently mounted using Eukitt™ mounting medium. Slides were dried, photographed, and analyzed with an Axio vision rel 4.8 light microscope Zeiss imager m2.

3.1.2.2.13. DAPI nuclear staining

DAPI (4',6-Diamidino-2-Phenylindole, Dihydrochloride), a nuclear and chromosome counterstain. The slide mounting was done adding a drop of DAPI into the slide with the paraffin sections of the WM-ISH samples. Added mounted cover slip, pressed gently and sealed the cover slip around with nail polish. The mounted preparations were allowed to air dry for 5 min before taking pictures.

3.2. *Amphiura filiformis*

3.2.1. *Animal collection and stabling condition*

Specimens of *Amphiura filiformis* were collected by Peterson mud grabs at a depth of 25-40 m from near the Seven Loven Centre for Marine Sciences, Kristineberg, on the Gullmar fjord, Sweden on September 2013. *A. filiformis* was sieved through the mud among other organisms for exclusive selection of the species. Approximately 1000 individuals were collected and placed in tanks with running deep water from the ocean keeping very similar environmental conditions (at 17°C). The animals were left to acclimatize in the lab for one week before used.

3.2.2. *Regeneration experiments on explants*

Explant samples were prepared, cutting suitable arm segments (1 cm from the disk and 1 cm after the first cut) using a scalpel and not inducing autotomy reaction. All double-amputated explants measured 1 cm in length. The explants were then placed in beakers with running deep water from the ocean at 17°C for established periods corresponding to prefixed repair-regenerative stages (0 d, 1 d, 3 d, 5 d, 7 d, 18 d, 30 d, 39 d).

3.2.2.1. Fixation

After each established collection stages, explants were anaesthetized with MgCl₂, then fixed with 2% Glutaraldehyde in 85% SW for 2 h at 4°C. Samples were then placed in FSW overnight at 4°C. Then the samples were processed for microscopy according to the specific methodology required (for SM, SEM, LM).

3.2.2.2. Stereomicroscopy (SM)

Standard methods for morphological analysis by stereomicroscopy (Leica MZ75, with Leica CLS 150XE lights, provided with a camera Leica Digilux 18.102) were employed. Photographs of both the distal and proximal explant ends were provided for all stages from 0 days to 39 days.

3.2.2.3. Scanning electron microscopy (SEM)

For SEM observations in *A. filiformis*, methods and protocols are those described in detail above (see pag 2). Repair and regenerative processes were analyzed in both proximal and distal ends of the explant samples from 0 days to 39 days.

3.2.2.4. Light microscopy (LM)

Samples fixed in 2% Glutaraldehyde (see above) were post-fixed with 1% osmic acid in 0.1 M cacodylate buffer (pH 7.2) for 2 h. Resin embedding was possible since *A. filiformis* arms are thin and not very calcified. For this reason, no decalcification procedure was used with these samples. After standard dehydration in an ethanol series, the samples were embedded in Epon 812-Araldite. For histological analysis, semi thin sections of 0.99 µm were cut with Reichert Ultracut E with glass knives, placed in glass slides, stained with crystal violet and basic fuchsin and observed under a Jenaval light microscope provided with a camera Panasonic GP- KR222.

3.3. Other comparative models: Ophioderma appressa and Ophioderma cinerea

3.3.1. Animal collection and stabilizing conditions:

Specimens of both species were collected at Inca Santa Marta Colombia with an average temperature of 27°C and brought to the lab in Bogota to an altitude of 2600 m with an average temperature of 14°C (but with sudden dramatically changes in temperature throughout the day). The change in altitude and temperature made it very challenging to keep the animals alive. Lastly, after two sample collection with several set up environmental conditions, animals were established in the aquarium with 1.025 salinity and 24°C water temperature, these latter appearing to be the main conditions affecting initial survival. Animals were fed with krill and calamari every week.

3.3.2. Regeneration experiments in the alive models

Molecular analyses were done only in *O. appressa* since it was the most abundant specie collected. In both *O. cinerea* and *O. appressa* specimens, arm regeneration was followed in eight animals during twelve weeks. The specimens were photographed once a week using a conventional stereomicroscope. Animals were anaesthetized with MgCl₂ before the pictures were taken.

3.3.3.1. DNA extraction: DNA was obtained by the phenol chloroform extraction method and used for amplification and isolation of SOXB1.

3.3.3.2. Degenerate primers design and cloning: Degenerate primers were designed with the alignment of the SOXB1 gene sequences, focusing on the most conserved regions of all echinoderms, some deuterostomians, and *Drosophila*. After alignment of all sequences primers were generated from the most conserved regions Frw: 5'-ATGAAYGCNTTYATGGTNTGG- 3', Rvs: 5'-RTANCCRTTCATRTANCCRTT-3'. With this primers SOXB1 was succesfully cloned

4. Results and Discussion

4.1. *Ophioderma longicauda*

4.1.1. Morphological Analysis

4.1.1.1. Scanning electron microscopy (SEM)

Arm regeneration in *O. longicauda* was monitored for an overall detailed morphological analysis. The arm amputations were performed by mimicking the conditions of autotomy mutilations (see Materials and Methods). The regenerative process was approached focusing on repair-regenerative development at the distal end, up to 12 weeks post-amputation (p.a): in particular, samples of 0, 1, 3 days and 1, 3, 6 and 12 weeks (p.a) were analysed by Scanning Electron Microscopy (SEM) (Fig. 4). The overall description provided below is the result of a comparative analysis of a number of samples carried out by comparing observations at SEM and Stereomicroscopy (SM) and integrating them with light microscopy (LM) data available in literature (Biressi *et al.*, 2009). This morphological characterization will help to better define the characteristic features of the regenerating arm in terms of external microscopic anatomy during the crucial stages of regeneration and to integrate them in a comprehensive view with all the different histological results previously obtained in *O. longicauda*.

0 day p.a. Shortly after the autotomy event the wound surface did not show any sign of repair processes. Since amputation was a real autotomy process (self-amputation), the stump was characterized by a strongly concave surface, only partly protected/covered by the prominent edges of the external skeletal shields.

1 day p.a. After 24 hours p.a, the autotomy surface showed the start of a cicatrization process characterized by an incomplete centripetal growth of a thin epithelial layer proceeding from the outer to the central-oral area. In the middle of the autotomy surface, the exposed vertebral ossicle was well visible: the ossicle structure was intact, confirming the conditions of autotomic amputation of the specimen.

3 days p.a. After 3 days p.a, the wound surface was covered by a well-developed continuous epithelial layer. This was supported by a loose stroma of fibrous connective tissue, well visible through the rips of the thin epithelial layer, often damaged by the fixations process.

1 week p.a. After 1 week p.a, the autotomy surface appeared to be healed by a conspicuous and thick cicatricial layer consisting of an outer thin epithelium and a dense inner layer of fibrous connective tissue. A regenerative bud started protruding from the center of the healed stump. Better seen in detail, autotomy surface showed a swelling bud slightly emerging in its central-oral area.

3 weeks p.a. After 3 weeks p.a, the regenerative bud was sufficiently developed to clearly emerge from the superficial arm shields with a morphological structure more defined.

6 weeks p.a. After 6 weeks p.a, the regenerating arm showed an obvious increase in size and a more prominent and elongated shape with recognizable developing spines. More in detail, the small regenerative arm appeared to be subdivided into two portions. The apical (distal) portions maintained a rather undefined structure and undifferentiated features comparable to those of the regenerative bud of the 1 week stage. In contrast, the basal (proximal) portion was well differentiated, and characterized by complete functional segments equipped with external appendages (spines) and covered by shields. According to the detailed histological studies by Biressi *et al.* (2010), at this stage the inner anatomy of the basal portion of the regenerating arm already achieved an advanced level of tissue differentiation detectable in all the main continuous structural components of the arm (radial nerve cord, coelomic canals and epineural sinus).

12 weeks p.a. After 12 weeks p.a, the regenerating arm looked like a well-differentiated miniature arm, at least as far as the proximal region of the regenerate is concerned. External skeletal shields, in many cases provided with developing spines, could be recognized. The histological analysis of the proximal regenerate region showed an high level of differentiation of the external structures, thus reflecting the situation of the internal anatomy in terms of tissues and organs. In contrast, the tip of

the regenerating arm still consisted of a regenerative blastema-like structure showing undifferentiated features.

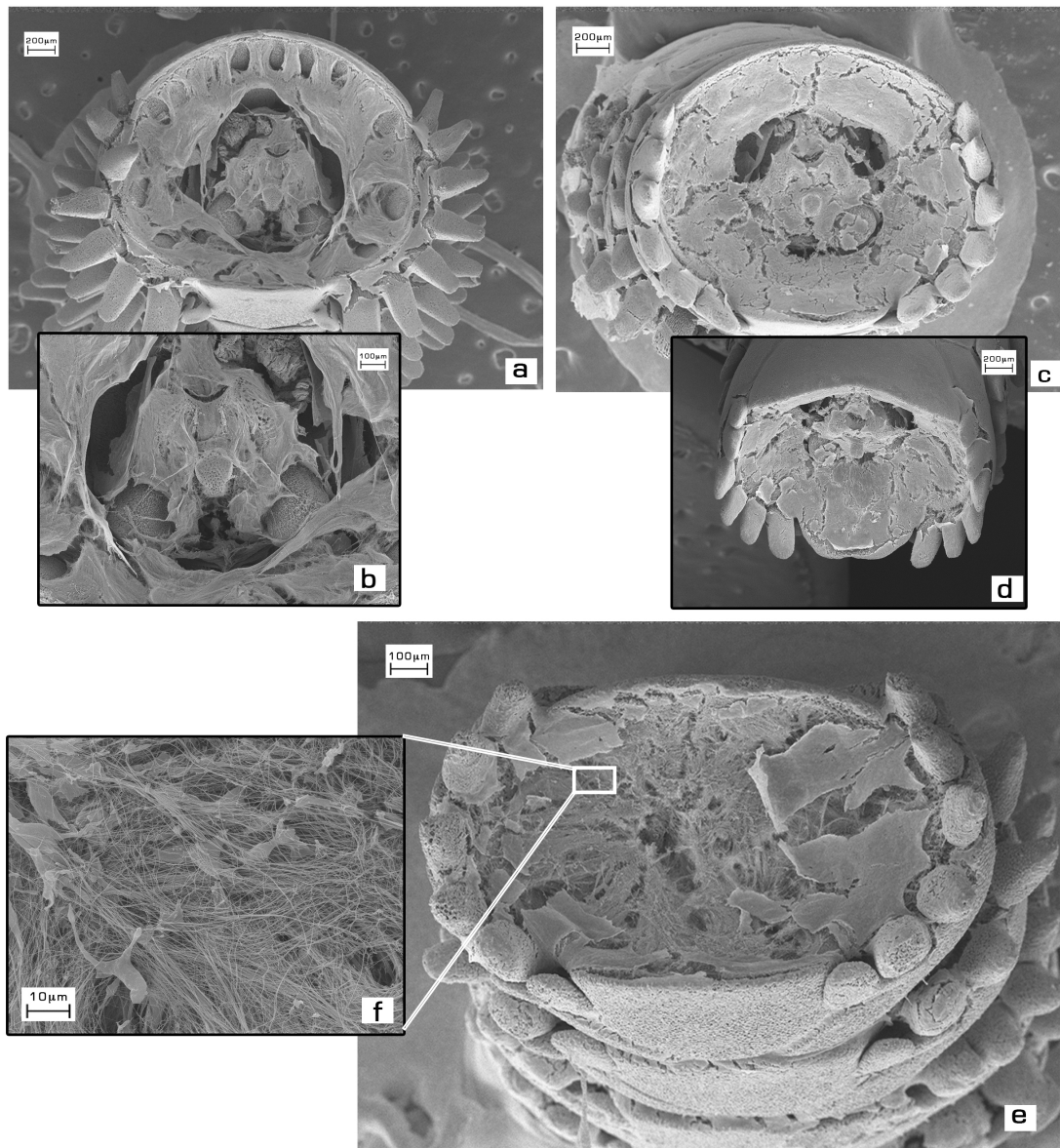


Figure 10. *O. longicauda*. SEM views of the stump and the regenerative arm (0h – 3 days). External morphological characterization of the different repair and regenerative stages after induced autotomy. Wound healing and arm regeneration are shown from a recent autotomized arm (0 day) up to 3 days pa (post-autotomy). (a-f). **a:** 0 dpa. The wound surface does not show any sign of repair. The injured tissues are exposed. **b:** detail of the surface with no sign of repair. **c,e:** 1 and 3 dpa. At these early stages, the amputation surfaces looked covered by a thin epithelial layer progressively becoming a continuous epithelium. **d:** detail 1 day after amputation showing the concavity of the segment after self amputation. **f:** detail of collagen fibers.

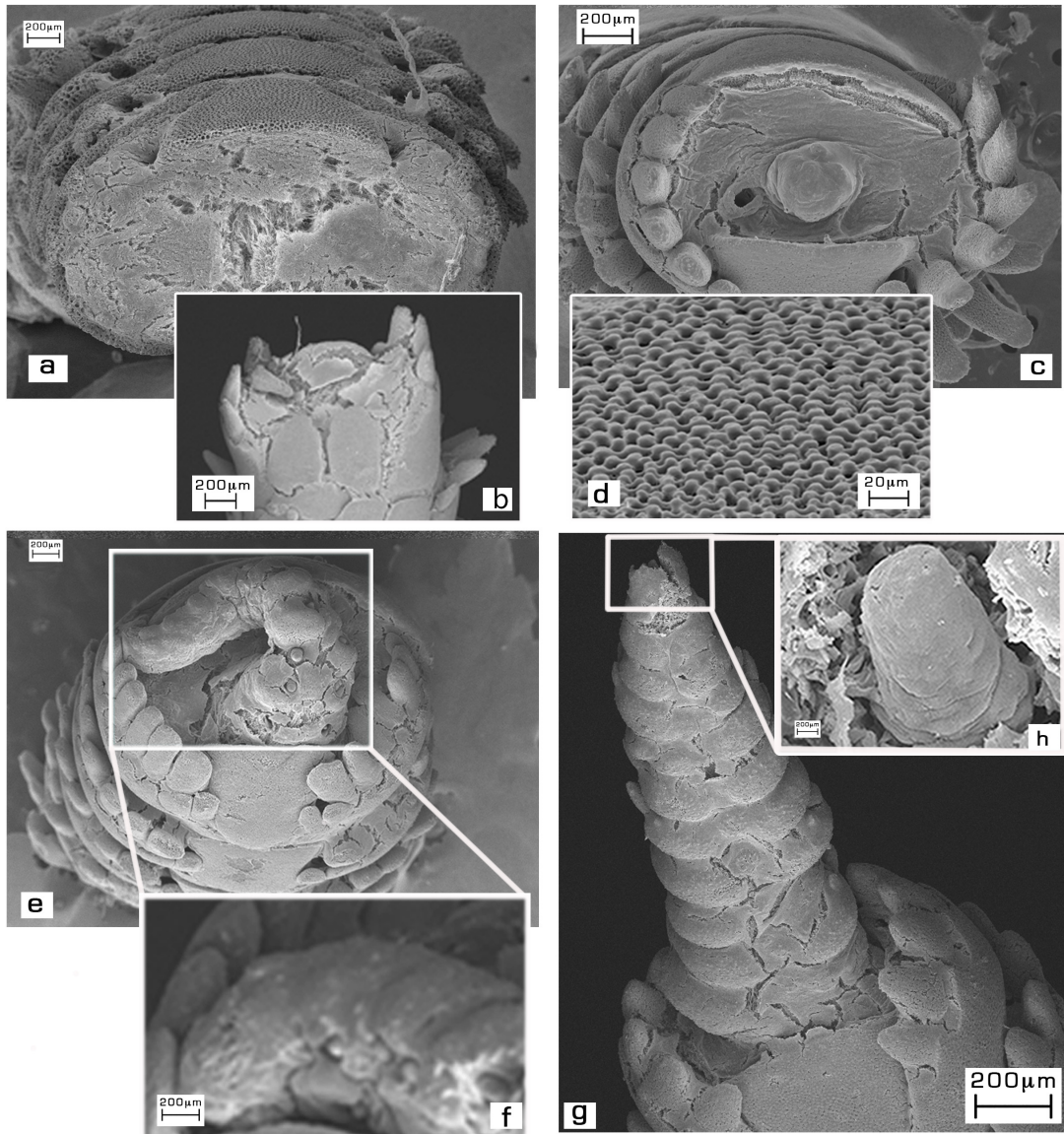


Figure 11. *O. longicauda*. SEM views of the stump and the regenerative arm (1 to 12 weeks). External morphological characterization of the different repair and regenerative stages after induced autotomy. Wound healing and arm regeneration are shown from 1 to 12 weeks pa (post-autotomy) (a-g). **a,b,c:** the amputation surface shows the early appearance of a regrowing blastema-like bud. **d:** detail of the stereom microstructure of the aboral shield of the stump. The structure is comparable to that of an intact shields. **e:** The regenerative arm is now visible: the regenerative part tend to be bend and adherent to its stump protected by spines and shields (also in fig 21c). **f:** detail of the undifferentiated apical part. **g:** The regenerating arm is progressively developing: during its growth it showed a more differentiated basal part, with an evident segmentation, and an undifferentiated apical part. Developing spines are present in the basal portion. **h:** detail of the undifferentiated apical part. *Note: the treatment for SEM preparation often can cause local damages or distortions of the samples*

SEM morphological results obtained in regenerating arms of *O. longicauda* analyzed from time 0 up to 12 weeks p.a can be compared to previous histological observations obtained by employing semithin sections studied for the same regeneration period (Biressi *et al.*, 2009). As expected, since the amputation was performed by reproducing autotomy conditions in all experiments, the main aspects of the regenerative processes turn out to be highly similar in terms of anatomical features, growth, and rate development. Based on these results, it can be easily inferred that the cellular mechanisms implied correspond to those previously described by (Biressi *et al.*, 2009). From a morphological point of view, the complete regenerative process, in terms of representative stages from the early post-autotomic stage to the development of a miniature functional arm complete in all its anatomical features, is confirmed to be subdivided into four main phases in *O. longicauda*: a repair phase, an early regenerative phase, an intermediate regenerative phase and an advanced regenerative phase.

The **repair phase**, which covers a p.a. period up to 3 days, is essentially characterized by wound-healing processes. These processes include early rearrangement of tissues involved directly in the autotomic process and emergency sealing of the structures. The presence of an incomplete and fragile cicatricial layer, formed by a thin outer epithelium only partly supported by an inner loose connective tissue stroma, often discontinuous, clearly indicates that the healing process is still largely incomplete at this stage (Fig. 10a, b, c, d).

The **early regenerative phase**, which covers the 3 days to 1 week p.a. period, is characterized by the end of the emergency healing and the start of true developmental regenerative processes. During this phase, the repair processes are completed and the wound is covered by a continuous cicatricial layer; the regeneration phenomena are limited to first signs of forward development expressed in a localized growth-center which can be considered a blastemal area (Fig. 11 e, f).

The **intermediate regenerative phase**, which covers from 1 week to 3 weeks p.a. period, is characterized by the formation and development of a well recognizable blastema-like bud. This grows forward from the oral part of the autotomy surface: both stump and regenerate look covered by a well-defined outer epithelium (Fig. 11g).

The **advanced regenerative phase**, which covers from 3 weeks to 12 weeks p.a., is a period of extensive growth, morphogenesis and differentiation which leads to the formation of a miniature arm. During this phase the external anatomy and the histological pattern of the regenerative arm become both progressively more defined: the regenerate basal (proximal) portion, in particular, acquires the distinctive internal and external features of a complete functional arm, whereas its apical (distal) portion looks rather undifferentiated and retains typical blastemal features. The regenerate growth continues in terms of length, as well as progressive differentiation of new structures. The regenerated arm maintains a different size and color with respect to the old stump for all the considered period of 12 weeks (Fig. 11i, j, k). It will reacquire its original size, becoming undistinguishable from the remaining non-regenerating arm, only after many months.

Overall, the sequence of events and processes seen in *O. longicauda* and employed in both repair and regenerative phenomena are rather comparable with those described in other species of ophiuroids already studied (Biressi *et al.*, 2009) supporting the idea of a common regenerative pathway in this group, which, although very versatile and species-specifically plastic, remains uniform in its basic mechanisms and features.

4.1.2. Molecular biology

In order to identify genes with a role in regeneration, a gene expression analysis has been performed during arm regeneration in the ophiuroid *O. longicauda*. cDNA subtractive suppression hybridization (SSH) library was constructed from regenerating (24 h) versus non-regenerating arms (0 h). This specific procedure has been chosen due to the complete lack of sequence information regarding the ophiuroid under investigation, not allowing the employment of the top-notch RNA-seq technology. The SSH technique enables specific cloning of expressed sequence tags (ESTs) representing genes that are differentially expressed in different mRNA populations and isolates genes without prior knowledge of their sequence or identity. It uses common molecular biological techniques that do not require specialized equipment or analyses. This method was very useful in screening new genes and construction of cDNA library. Given the current understanding of regeneration in ophiuroids at the molecular level, this technique is a suitable method for the detection

of low-abundance, differentially expressed transcripts that can lead to the isolation of putative tissue remodeling and repair phase of regeneration related genes.

From this library several cDNA clones have been singled-out, and some of them sequenced. The most promising ones were selected for further analyses on the basis of their similarity to genes already characterized in other model systems, especially DO3 which has a homolog with an echinoderm. The genes selected were labeled as CO3, DO3, FO3, GO3 with the following homologies written below.

CO3: emb|AJ580250.1| *Vipera berus berus* mRNA for ammodytin L(2) variant, (AmL(2)), known to secret phospholipases A₂ (sPLA₂s). They are abundant in snake venoms. The molecular mechanisms underlying these effects are still poorly understood. Although, Connolly et al. reported features consistent with axonal regeneration and the re-innervation of denervated muscle fibers (Kularatne, 2002). Though, at this point whether regeneration is sustainable in the long term is difficult to judge (Connolly *et al.*, 1995).

DO3: XM_003724813.1 *Strongylocentrotus purpuratus* dnaJ homolog subfamily C member 7-like (LOC585533), mRNA. Roles for DNAJ family and DNAJC7 involvement in regeneration have been previously reported during early liver human regeneration (Wolf *et al.*, 2014). In zebrafish the protein plays a role during fin regeneration (Tawk *et al.*, 2000). In mouse, DNAJC7 has been shown to interact with RAD9A, a cell cycle checkpoint protein required for cell cycle arrest and DNA damage repair in response to DNA damage (Wolf *et al.*, 2014).

FO3: emb|AJ580282.1| *Vipera aspis aspis* mRNA for vaspin basic subunit variant, (Vasp B) Vasodilator-stimulated phosphoprotein (VASP) is expressed in many different cell types but is especially prominent in platelets, smooth muscle cells, and vascular endothelial cells. Ena/VASP proteins are involved in crucial cellular functions, such as shape change, adhesion, migration and cell-cell interaction (Pula *et al.*, 2008). VASP was associated in mice with remarkable capillary preservation/regeneration up to day 28 mediated via an increased proliferative and a reduced apoptotic activity (Hohenstein *et al.*, 2005)

GO3: gb|EU558534.1| *Arabidopsis lyrata* clone SINE9 transposon-insertion display band genomic sequence. Short Interspersed Nuclear Elements (SINE) are short DNA sequences (<500 bases) that represent reverse-transcribed RNA molecules originally transcribed by RNA polymerase III into tRNA, 5S ribosomal RNA, and other small nuclear RNAs. SINE 9 seems to be associated with Type I retrotransposons that have phenotypes which suggest they are involved in regeneration of germ cells (Slotkin & Martienssen, 2007)

DO3: DNAJC7 ortholog in *O. longicauda* (*OIDNAJC7*).

341 bp of this clone were sequenced and matched to the 3'UTR region of the *Strongylocentrotus purpuratus* DNAJ, subfamily C member 7-like (DNAJC7) mRNA (79% identity). This protein has been previously demonstrated having roles in regeneration in other biological models (Tawk *et al.*, 2000). *S. purpuratus* mRNA is 8224bp long, and encodes a protein of 467 aminoacids (Fig.12). DNAJC7 ortholog in *O. longicauda* was thus named *OIDNAJC7*.

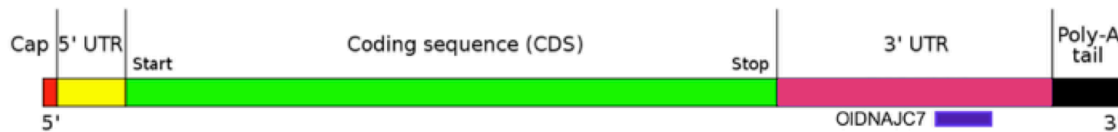


Figure 12. Structure of the *Strongylocentrotus purpuratus* DNAJC7 (SpDNAJC7) mRNA and position (from nucleotide 6128 to nucleotide 6686 of SpDNAJC7) of the cDNA fragment of *O. longicauda*, singled-out in this study.

OIDNAJC7 ortholog clone was used to generate a probe to perform *in-situ* hybridization (ISH) in two different parts of the arm, (middle and tip) at two different regenerating stages (24 h and 48 h) and a non-regenerating (0 h) one, with no clear difference in expression among all samples (Fig. 12). This ISH methodology was optimized for this model using the *O. longicauda* 18S gene as a control probe. To isolate the fragment of 150bp of the *O118S* gene we designed a pair of primers based on the multiple alignment of several 18S genes from different species, from fly to high Vertebrates (see Material and Methods for sequences).

Expression of *OIDNAJC7* antisense probe revealed a pattern along the oral side of the arm in the RWC in both regenerating and non-regenerating arms in the middle and tip of the arm, at the two regenerative time points (24 h and at 48 h), and at time 0 (non-

regenerating) (Fig. 13). Expression was seen at each segmental interval at the bases of the tube feet pair occurring in the lateral and radial water canal (RWC). This staining pattern was not seen in arms treated with the *OIDNAJC7* sense probe (Fig. 14). Eight μm wax sections of regenerating and non-regenerating arms indicated that this *OIDNAJC7* antisense probe staining is also present in the ectodermal layer covering the coelomic cavity (Fig. 13 D-H).

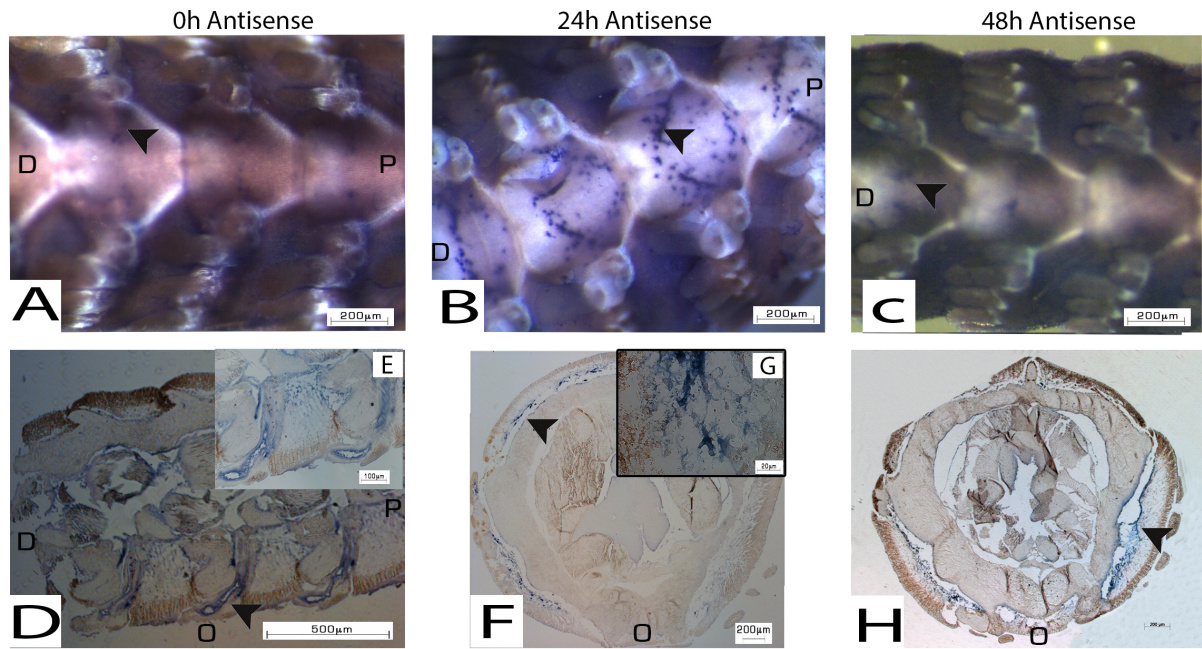


Figure 13. *In-situ* detection with antisense (AS) probe of *OIDNAJC7* (A-H). *OIDNAJC7* expression was determined by WMISH (A-C) and in 8 μm wax color developed sections (D-H). (A, D-E): 0 h; (B, F-G): 24 h; (C, H): 48 h after amputation. The signal is indicated with a black arrowhead and orientation by O oral, D distal, P proximal.

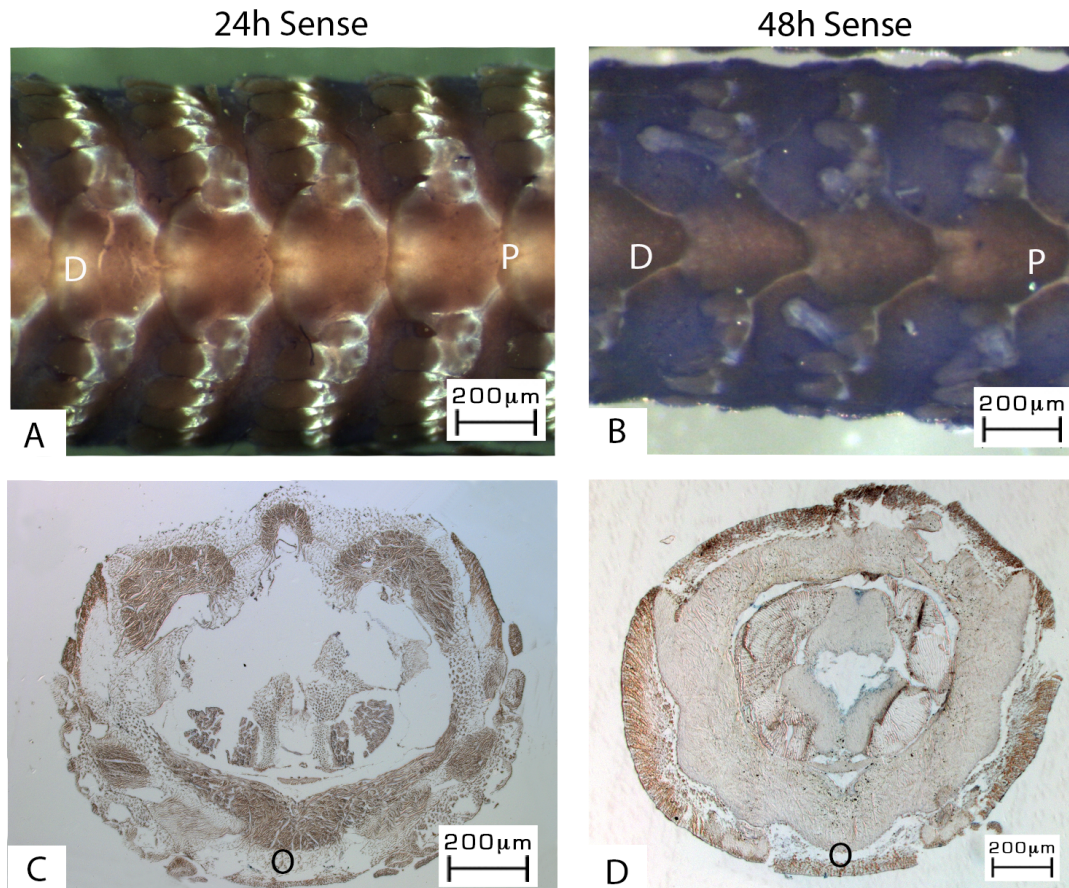


Figure 14. *In-situ* with sense probe of *ODNAJC7* (A-D). *ODNAJC7* sense probe was used as control. As expected, no expression was detected by WMISH (A-B) and in the 8 μm wax sections obtained from the WMISH (C-D). (A, C): 24 h; (B, D): 48 h after amputation. O oral, D distal, P proximal.

Roles for DNAJ family and DNAJC7 involvement in regeneration have been previously reported in the literature. Hsp 70 functions as a chaperone during periods of cellular stress and induces the expression of several inflammatory cytokines identified as key players during early liver regeneration (Wolf *et al.*, 2014). In zebrafish the protein plays a role during fin regeneration, showing drastically increased in all ray segments beneath the regenerated part, or blastema, in response to caudal fin amputation (Tawk *et al.*, 2000). In mouse, *DNAJC7* has been shown to interact with RAD9A, a cell cycle checkpoint protein required for cell cycle arrest and DNA damage repair in response to DNA damage (Wolf *et al.*, 2014).

This staining pattern was not seen in arms treated with the *ODNAJC7* sense probe. This information, together with the ISH results, could suggest a putative role for

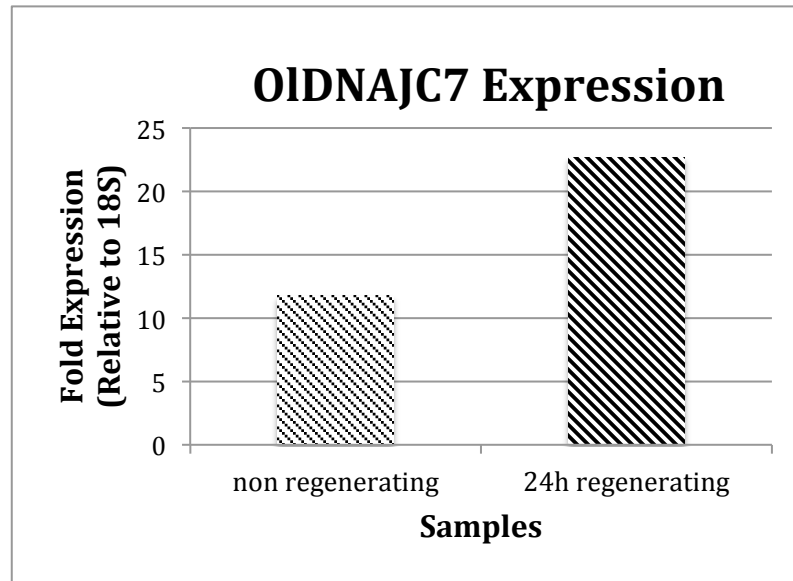
OIDNAJC7 during arm regeneration in *O. longicauda*. Moreover, due to the fact that *DNAJC7* contains tetratricopeptide repeats known to be involved in cell cycle control (Tawk *et al.*, 2000), it is likely that the role of this protein during *O. longicauda* arm regeneration could be based on its ability to regulate cell proliferation.

Expression of *OIDNAJC7* in regenerating and non-regenerating arms in the coelom and RWC

Interestingly, *OIDNAJC7* mRNA was detected at the bases of the tube feet pair associated with each segment occurring in the lateral and radial water canal (RWC) at the oral side along each segment of the regenerating and non-regenerating arms. A compartment of the coelom is transformed into a unique water-vascular system that uses hydraulic power to operate a multitude of tiny tube feet that are used in locomotion and food capture. Based on this evidence, it is suggested that the coelomic epithelium that lines the RWC may be a key source of cells used in the ophiuroid regenerative process.

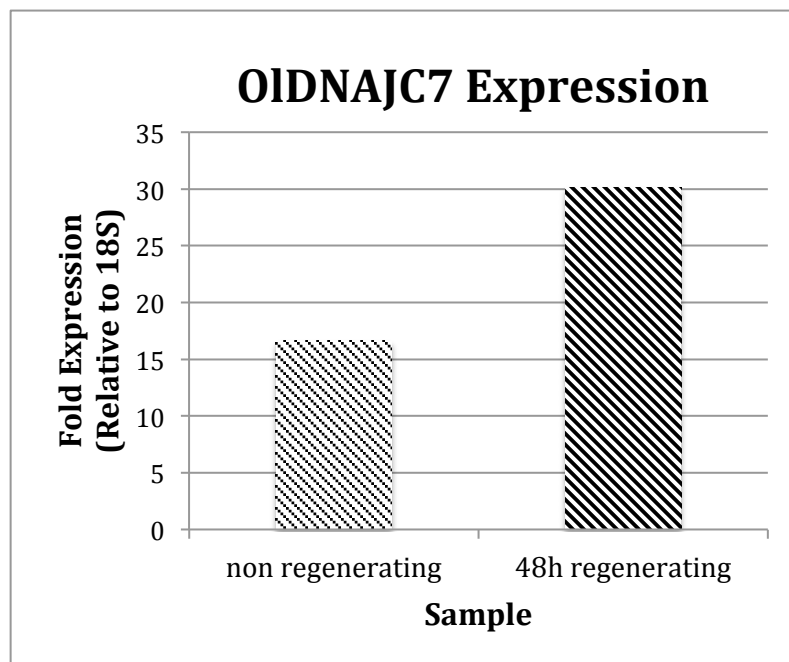
Since this is the first time that *DNAJC7* is reported in an echinoderm with a putative implication in regeneration it cannot be compared with other close organisms. Therefore, one possible explanation for the regular segmental intensity of *OIDNAJC7* may be that these areas of high message levels represent segmental pools of cells set aside and ready for use in arm regeneration. Such a system may well be beneficial to this species due to the high incidence of epimorphic arm regeneration, *i.e.* undifferentiated cells migrate to the autotomy site and form a regenerative bud or ‘blastema’; (Thorndyke *et al.*, 2001) that occurs naturally in this species (Sköld & Rosenberg, 1996). These segmental pools would provide a source of cellular material close to the autotomy plane, where breakage occurs along the length of the arm. The present study adds to the increasing evidence for the importance of the echinoderm coelom as a source of set-aside cells for the regenerative development in adults. This hypothesis further implies a key role for the coelomic RWC as a source of cellular material for use in ophiuroids arm regeneration.

Interestingly, the level of *OIDNAJC7* mRNA resulted increased in regenerating arms in comparison to control at both 24 h (Fig. 15) and 48 h (Fig. 16) following amputation.



Sample	18S	OIDNAJC7	Delta Ct	Folds (100000)	Value
non regenerating	13,7	26,755	13,055	0,0001175	11,75042
24h regenerating	16,13	28,235	12,105	0,000227	22,700316

Figure 15. qPCR analysis of OIDNAJC7 gene after 24 h regeneration relative to 18S.



Sample	18S	OIDNAJC7	Delta Ct	Folds (100000)	Value
non regenerating	14,2	26,755	12,555	0,0001662	16,617604
48h regenerating	16,54	28,235	11,695	0,0003016	30,161588

Figure 16. qPCR analysis of OIDNAJC7 gene after 48 h regeneration relative to 18S

Significance of HSP 70 and *OIDNAJC7* in echinoderm regeneration

There is continuous *OIDNAJC7* expression observed in presumptive coelomocytes all along the RWC of the regenerating and non-regenerating arm, and this is appreciably distributed at regular segmental intervals along the oral length (Fig. 13). The organogenetic potential of the echinoderm coelom has been recognized for some time now. Indeed, in their review, Candia Carnevali and Bonasoro (2001) suggested such a functional possibility for this structure. It is also possible that the cells expressing this mRNA in the regenerating arm originated in the RWC, that it has been previously describe to be a source of circulating cells, the coelomocytes (Chia & Xing, 1996; Smith, 1981). Also, it has been shown in wounded echinoderms that coelomocytes accumulate rapidly and perform a local clotting reaction to prevent loss of coelomic fluid (Smith, 1981). According to Pinsino and co-workers (Pinsino; *et al.*, 2006; Pinsino *et al.*, 2007) the trend in the total coelomocyte count (TCC) in the steroid *Asterias rubens* increases at 1–6 h after wounding. In addition, coelomocytes from trauma-stressed animals showed a time-dependent increase in Hsp 70 levels, as detected by both immunocytochemistry and immunoblotting within 24 hours after arm tip amputation, with a peak at 6 hours after amputation. The increment of Hsp 70 during trauma could suggest a function of it as a chaperone during periods of cellular stress (as in human liver) such as amputation and could be inducing the expression of several inflammatory cytokines in ophiuroids hence, showing an up regulation of this protein during regeneration, in agreement with the increased in *OIDNAJC7* gene expression reported in the present study.

In sea urchin Hsp 70 has shown increased in levels of coelomocytes in response to temperature stress, acidic pH, heavy metals, and other pollutants (Matranga *et al.*, 2006). Furthermore, the function of Hsp proteins in a number of intracellular processes, such as chaperone guidance (Becker & Craig, 1994) protein folding (Buchner, 1996), and protection against apoptosis (Parcellier *et al.*, 2003), might explain their high evolutionary conservation and the presence of *DNAJC7* in regenerative arms.

This, together with their up regulation during cellular stress, makes them an important part of both the defense and immune systems. Similarly, in armed echinoderms, Hsp 70 has been shown to be involved in autotomy and wound repair, with a putative

function in tissue remodeling and associated protein turnover during regeneration (Patrino *et al.*, 2001). Hence, it can be hypothesized that DNAJC7 in *O. longicauda* could play an important role in Hsp 70 regulation during early regeneration in echinoderms indicating a putative role for coelomocytes and classic stress molecules in the post-traumatic stress associated with the early repair phase of regeneration.

4.2. *Amphiura filiformis*

4.2.1. *Microscopy*

Double amputated explants of *A. filiformis*, analyzed for 39 days after amputation, showed 100% vitality throughout the whole period, responding to luminosity, chemical and mechanical stimuli and maintaining the capacity to explore the environment by podia. An overall morphological analysis of the regenerative process in these explants was approached focusing on repair-regenerative development at both the distal and proximal ends for 39 days in order to show the different polar growth at very early and advanced stages. The performed integrated analysis included stereomicroscopy (SM, Fig. 17), scanning electron microscopy (SEM, Fig. 18) and light microscopy (LM, Fig 19, 20). The overall morphological description provided below is the results of a comparative analysis of a number of samples carried out by employing all these different methods and putting together the different results in a comprehensive view.

In terms of general morphology and external features, much information could be obtained from specimens observed at SM and SEM. In terms of tissue and cell pattern, essential details could be derived by comparing suitable histological sagittal sections, in particular semi thin resin sections of individual samples of proximal and distal explant portions. Distal or proximal samples could be always easily identifiable in the sagittal plane by observing the orientation of distinctive features such as shields, tube feet, and/or spines (oriented towards the wounded side in the distal portions, and in the opposite direction in the proximal portions).

4.2.2.1. Stereomicroscopy (SM), scanning electron microscopy (SEM) and light microscopy (LM)

0 day p.a. Right after amputation, both distal and proximal ends of the explant did not show any sign of repair processes. The amputation surfaces looked very irregular: on the exposed skeletal tissue the stereom pattern was recognizable and only some tissue remains were present, most of all bundles of intervertebral muscles involved in the cut. The other anatomical structures looked to respond to the trauma to a different extent: in particular, all the main coelomic compartments underwent a sort of coarctation closing their open ends; these sealed parts of the canals provided a partial cover for the injured end of the nerve cord which appeared to be rather retracted and not exposed outside. Close to and far from the amputation area, groups of cells identifiable as migratory elements such as coelomocytes (small elements with scarce cytoplasm) and phagocytes (large cells with irregular profiles and evident cytoplasmic inclusions) could be detected inside the coelomic canals and in the adjacent connective tissues.

1 day p.a. After 24 hours p.a, at both the explant ends, the amputation surfaces looked partly covered and protected by the terminal skeletal shields, respectively the most distal and the most proximal ones, which tended to bend over the amputation surface. As a consequence, the overall profile of both the explant ends appeared significantly modified and restricted with respect to the central portion. This was due also to the effects of the general coarctation of all the terminal parts of the coelomic compartments whose walls tended to collapse. In terms of microscopic anatomy, a first appearance of a new, very thin epithelial layer was already visible on both the amputation surfaces. The remains of the aboral muscle bundle involved in the amputation were well recognizable and showed a significant disorganized internal pattern. All the coelomic compartments were sealed off and repaired in their histological structure. The injured end of the nerve cord was still retracted and covered by the end of the radial water canal, which tended to be bent over. Both of these structures did not enter in direct contact with the new epithelial layer, a loose cicatricial layer of connective tissue maintaining them well separated from the amputation surface. As in the previous stage, migratory cells were frequently detectable inside the coelomic canals and in the connective tissue context.

3 days p.a. After 3 days p.a, both the distal and proximal wound surfaces were covered by a well developed epithelial layer now externally visible also at SM and SEM. The histological sections showed that the thin epithelium was supported by a continuous cicatricial layer of dishomogeneous connective tissue; fibers and cells were irregularly scattered and mixed to empty spaces. A conspicuous presence of remains of the aboral muscular bundles involved in the amputation was still present, the muscle pattern always showing a remarkable degree of disorganization in both the loose reciprocal arrangement of fibers and individual myocyte structure. A number of presumptive dedifferentiating myocytes could be recognized on the basis of their typical oblong shape and dark stain. As for the other structures, all the features described for the previous stages appeared to be emphasized. A massive cell migration could be detected inside all the coelomic compartments, where masses of cells were crowded around the walls of their distal ends.

5 days p.a. After 5 days p.a, the two sides of the explants changed significantly. At the distal end, an early appearance of a well recognizable regenerative bud was visible in the central-oral area of the amputation surface. In contrast, no sign of regrowth was observed on the proximal end, still characterized by the re-epithelialization of the wound surface and by the typical inclination of the aboral shield still bent over the amputation as in the earlier stages. In terms of microscopic anatomy, the distal bud showed a complex structure: it was covered by an outer pluristratified epithelium and consisted of a fibrous mesenchymal stroma in which the radial water canal, the perivisceral coelomic compartment and the radial nerve cords are regrowing. Massive groups of cells could be detected inside the different coelomic components, particularly the water canal, whose internal walls appeared to be involved in extensive proliferation processes often obliterating the lumen. The muscle remains as well as the intact muscles of the explant were clearly both subjected to an evident reorganization process characterized by progressive loss of bundle integrity and myocyte dedifferentiation.

7 days p.a. After 7 days p.a, the blastemal growth became very evident on the distal amputation, with a localized development of a more pronounced regenerative blastema at the level of the central-oral area, whereas the pattern was more or less

quite unchanged in the proximal end. The histological section confirmed that the blastemal regrowth occurred in correspondence with the neural cord and the radial water canal. The blastema complexity was more or less comparable to that characterizing the regeneration of the normal arm in this same species (Biresi *et al.*, 2009), a distinctive feature being the regrowth of the radial nerve cord associated to the outgrowth of the perivisceral coelom and the radial water canal. The apical part of the regenerating coelomic components, in particular, showed a “solid” structure mainly due to the massive presence of cellular aggregations, formed by coelomocytes, phagocytes and dedifferentiating myocytes. These same cytotypes were very often found free in all the coelomic canals and cavities far from the amputation, suggesting a massive cell mobilization/migration towards the regrowth region. As far as the muscles are concerned, they showed the same disarranged pattern already described in the previous stage.

18 days p.a. After 18 days p.a, the regenerate grown on the distal amputation acquired a more defined anatomy resembling that of a small arm, apart from the lack of the typical external appendages. In contrast, the proximal amputation continued to show only signs of repair, the cicatricial layer covering the wound surface looking thick and complete. In spite of the lack of developing spines and tube feet, the distal regenerate was rather developed in length and could be subdivided into two distinct portions, basal and apical. The basal portion showed an advanced level of differentiation: it was characterized by an evident segmentation process in progress, dominated by the outgrowths of 1) the radial nerve with an evident ganglionated structure; 2) the wide perivisceral coelomic cavities; 3) the radial water canal. The apical portion was instead characterized by a rather undifferentiated structure and maintained the blastemal aspect seen in the earlier stages (5-7 days pa). On its whole, the explant regeneration presented a significant delay in terms of development if compared to normal arm regeneration at this same stage (Biresi *et al.*, 2009).

30-39 days p.a. After 30 and 39 days p.a, the small regenerating arm was more developed. It was still subdivided into two portions. The basal (proximal) portion was well differentiated, and was characterized by complete functional segments equipped with all the external appendages (spines and podia) and covered by shields. The histological pattern was that typical of the adult arm, characterized by the

presence of: perivisceral coelom; radial water canal with podia; epineural sinus; radial nerve cord; vertebral ossicles; intervertebral muscles and ligaments; superficial skeletal shields. In contrast, the apical portion still maintained undifferentiated features. As far as the proximal amputation is concerned, this did not show any significant changes in terms of repair processes and no signs of blastemal regrowth was detectable. Interestingly, besides the evident regenerative growth at the distal end, the anatomical structure of the explant appeared to lose its integrity and compact pattern, the tissues more affected being the muscle bundles, which looked thinner, less defined and disorganized with respect to the explant original structure.

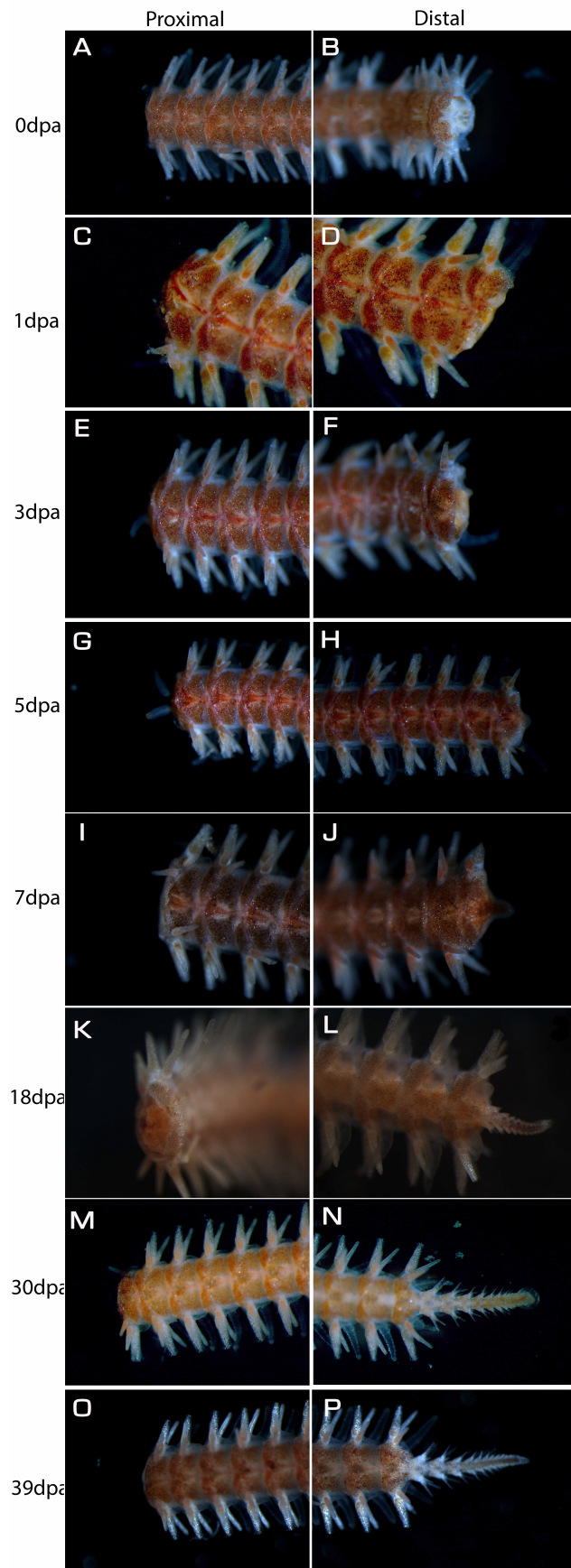


Figure 17. *Amphiura filiformis* explants: whole mount stereomicroscopy. Aboral view of the **distal (on the right)** and **proximal (on the left)** explant ends of *Amphiura filiformis* following double amputation. Wound healing and regeneration are shown from 0 to 39 dpa (days post-amputation) at both the ends (A-P).

A, B: 0 dpa. Both distal and proximal ends do not show any sign of repair. **C, D, E, F:** 1 and 3 dpa. At these early stages, the distal and proximal amputations start to be partly covered by the external shields, particularly the aboral one. **G, I:** 5 and 7 dpa. The distal amputation shows early appearance of a regrowing blastema. **H, J:** 5 and 7 dpa. No sign of regrowth is visible on the proximal amputation of both stages. **K, L:** 18 dpa. A very evident regenerate is developed at the distal end (K), whereas the proximal end does not show any sign of regrowth (L). **M, O:** 30 and 39 dpa. Distal amputations. The regenerating arm grows showing a more differentiated basal part, with an evident segmentation, and an undifferentiated apical part. Developing spines and tube feet are present in the basal portion. **N, P:** 30 and 39 dpa. Proximal amputations. No visible blastemal regrowth is present.

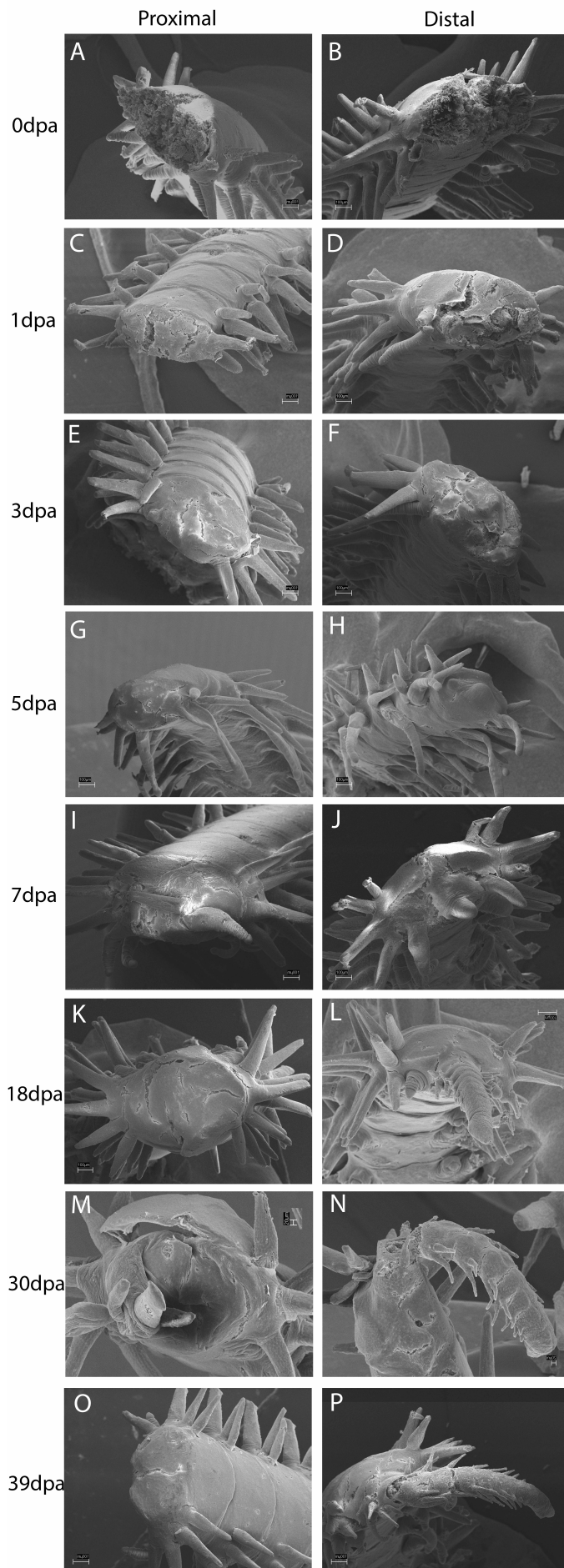


Figure 18. *Amphiura filiformis* explants: whole mount Scanning Electron Microscopy (SEM). Aboral view of the **distal (on the right)** and **proximal (on the left)** explant ends of *Amphiura filiformis* following double amputation. Wound healing and regeneration are shown from 0 to 39 dpa (days post-amputation) at both the ends (A-P).

A, B: 0 dpa. Both the distal and the proximal amputation surfaces show the exposed skeletal tissue of the vertebral ossicles, partly presenting remains of the intervertebral muscle bundles. **C, D:** 1 dpa. On both distal and proximal amputations, a new epithelial layer covers the entire wound surfaces. Aboral and oral shields are slightly bent towards the center of the arm to partly protect the wounded area. **E, F:** 3 dpa. D.

A small regenerative bud is developing in the distal end, in its central-oral area (**E**), whereas no appearance of regrowth is visible on the proximal end still characterized by a simple cicatrization (**F**). **G, I:** 5 and 7 dpa. Distal amputation. A clear regenerate is progressively developing. **K, M, O:** 18, 30, 39 dpa. Distal amputations. Regenerating arms at different stages are detectable. The regenerate basal part is acquiring its segmentation pattern. Spines and tube feet are progressively developed. The apical regenerate maintains a rather undifferentiated structure. **H, J, L, N, P:** 5, 7, 18, 30, 39 dpa. Proximal amputation at different stages. There is no sign of regrowth. A thicker cicatricial layer is covering the wound.

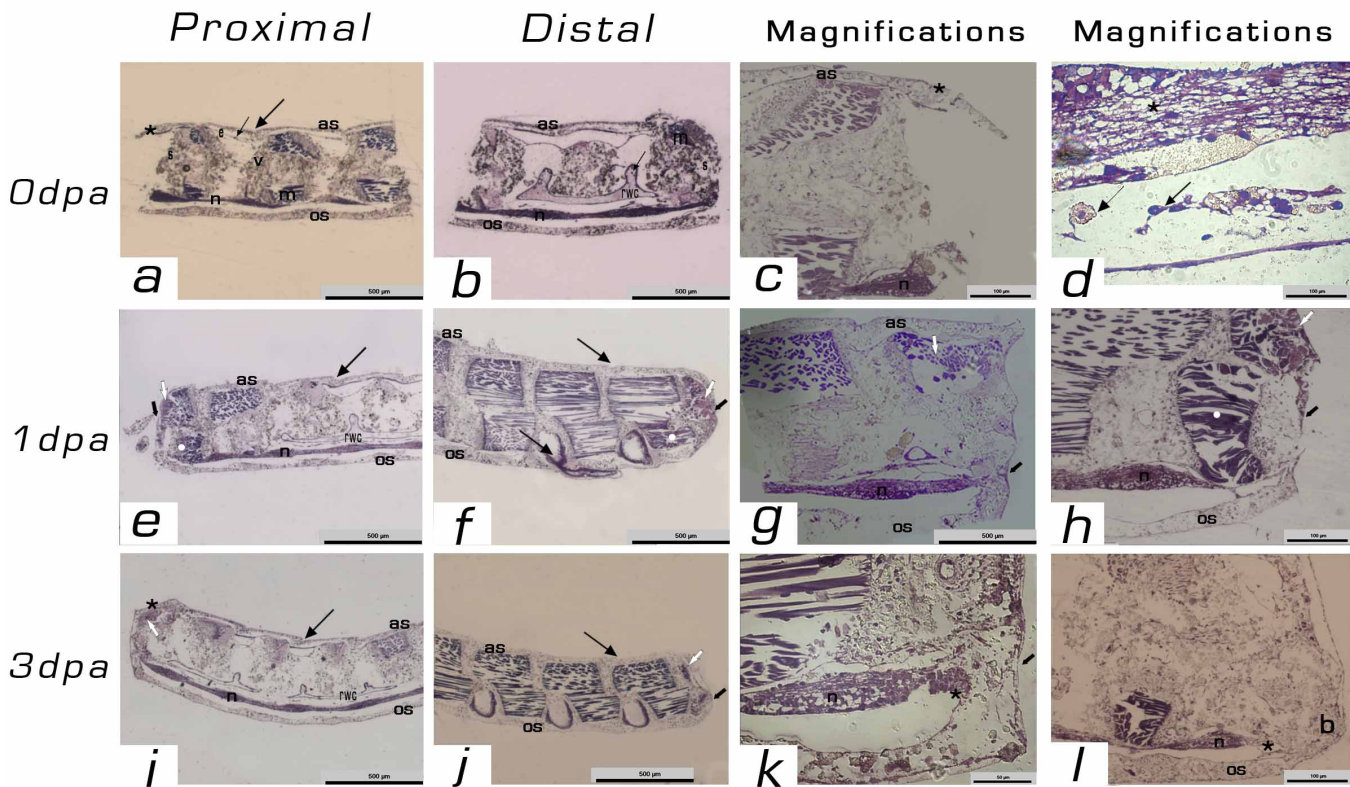


Figure 19. *Amphiura filiformis* explants: Light microscopy (LM) of semithin sagittal resin sections. Sagittal and cross sections of: proximal view (**first column on the left**) and distal view (**three columns on the left**) of *Amphiura filiformis* following double amputation. Wound healing and regeneration are shown from 0 to 3 dpa (days post-amputation) at both the ends (P-D). **a, b, c, d.** 0 dpa. **a, b:** P and D ends. Both P and D amputation surfaces do not show signs of healing and wide part of the stereom is exposed. **c:** detail of D end. The open wound is shown. Remains of injured muscles (*m*) are visible. Aboral shield (*as*) is bent, apparently for wound protection (*asterisk*). **d:** detail of D part of the nerve. Migratory cells can be found in the coelomic channel (arrows). **e, f, g, h.** 1 dpa. **e, f:** P and D ends. Both P and D amputations show a very thin epithelial layer (*thick arrow*) covering the wound area. The whole muscle pattern of the explant is shown in **f:** The aboral muscle close to the wound starts showing a disorganized pattern (*white arrow*). **g:** detail of D. View of the aboral muscles close to the wound involved in clear dedifferentiation processes (*white arrow*). Clear view of the thin epithelial layer (*arrow*) covering the wound area. **h:** detail of D. Dedifferentiation processes (*white arrow*) involved the muscle remains (aboral invertebral muscle) and to a minor extent the oral muscle closer to the wound (*white dot*). **i, j, k, l:** 3 dpa. **i, j:** P and D ends. Both P and D ends show their amputation surfaces covered by a thick cicatricial layer (*arrows*). On P side of the wound no signs of regrowth are visible. On D side a very small protruding bud is visible (*black thick arrow*). **k:** D detail showing the new epithelium (*thick arrow*) and the terminal sealed portion of the perivisceral coelom (*asterisk*). **l:** detail of D showing the terminal sealed end of the nerve cord and radial water canal (*asterisk*). Aboral arm shield (*as*), lateral arm shield (*ls*), oral arm shield (*os*), podia (*p*), spine (*s*), vertebral ossicle (*v*), radial

water canal (*rwc*), muscles (*m*), nerve (*n*), blastema (*b*) coelom (*c*), radial water canal (*rwc*) and epineural sinuses (*e*).

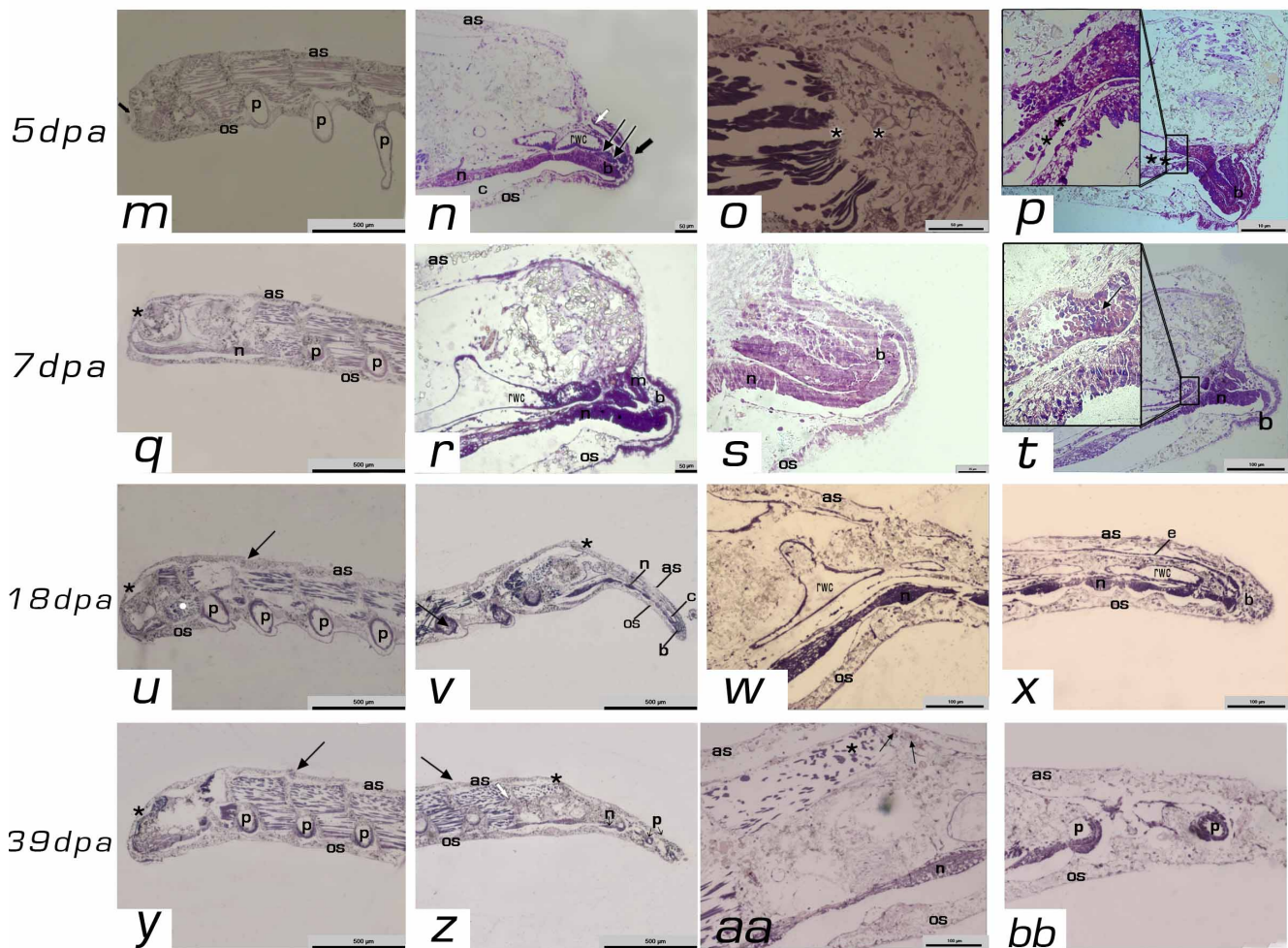


Figure 20. *Amphiura filiformis* explants: Light microscopy (LM) of semi thin sagittal resin section. Sagittal and cross sections of: proximal view (**first column on the left**) and distal view (**three columns on the left**) of *Amphiura filiformis* following double amputation. Wound healing and regeneration are shown from 5 to 39 dpa (days post-amputation) at both the ends (P-D). **m, n, o, p:** 5dpa. **m, n:** P and D ends. On P side the wound is entirely covered by a cicatricial layer covered by continuous epithelium: no signs of regrowth is visible (*thick arrow*). On D side a very small protruding bud is visible. The extension of the main coelomic canals (*c*), the nerve (*n*), the hyponeural (*h*) and epineural sinuses (*e*) are projecting into the blastemal mesenchymal stroma (*b*) **o:** detail of D. The aboral muscle close to the wound shows a highly disorganized pattern in both myocyte pattern and structure. **p:** detail of D. The wall of the terminal coelomic canals is crowded by proliferating coelomocytes (*double asterisk*), which detach and travel inside the lumen (*inset*).

q, r, s, t: 7dpa. **q, r:** P and D ends. On P side the wound still shows only a cicatricial layer (*thick arrow*). On the D side an evident progressive growth of the regenerate is evident (*b*). The distal ends of the perivisceral canals and the radial water canal (*rwc*) appeared to be hypertrophic and completely sealed off. Their walls are locally

thickened and often show massive phenomena of cell proliferation. **s**: D detail of the bud: massive accumulation of migratory cells are present in the mesenchymal matrix. **t**: detail of D end, showing local mobilization of migratory cells inside the radial water canal: coelomocytes, phagocytes and myocytes can be distinguished on the basis of their morphological features (**inset**). Apparently free elements can also be detected in the mesenchymal stroma in close association with the nerve (n), the radial water canal (rwc) and aboral muscle (m).

u, v, w, x: 18dpa. **u, v**: P and D ends. On P side the cicatricial layer is the same seen in q (*asterisk*). On D side a miniature arm is well developed with a recognizable and defined anatomical structure. **w**: detail of D end showing the stump and the basal portion of the regenerating arm. **x**: D side. Overall view of the well developed regenerating arm showing its internal differentiated structures: radial nerve cord, radial water canal, perivisceral coelom and apical blastema are clearly recognizable.

y, z, aa, bb: 39 dpa. **y, z**: P and D ends. On P side there is no signs of bud formation. On D side the regenerating arm is progressively developing in all its structural components, including podia (b). **aa**: detail of D end showing the stump and the basal portion of the regenerating arm. **bb**: detail of D. In the basal part of the regenerating arm D developing podia are found (p). Aboral arm shield (as), lateral arm shield (ls), oral arm shield (os), podia (p), spine (s), vertebral ossicle (v), radial water canal (rwc), muscles (m), nerve (n), blastema (b) coelom (c), radial water canal (rwc) and epineural sinuses (e). hyponeural sinuses (h)

The results obtained in the arm double-explants can be analyzed by comparing the explant model with the normal arm regeneration previously studied up to 26 days by (Biressi *et al.*, 2009) in *A. filiformis*. Due to the evident polar regrowth, the comparison is obviously possible only taking into account the explant distal amputation, since on its proximal amputation only repair processes could be observed. As expected, the regenerative processes occurring in the distal amputation were on the whole rather slower than those of the arm. Nevertheless, in terms of morphogenesis and differentiation processes, it was possible to find a certain correspondence between the regenerative stages of the two models (summarized in Table 4).

Table 4. Correspondence of regenerative stages between normal arm and explant of *A. filiformis*

Explant distal regeneration	Arm regeneration
1 dpa.	1 dpa.
3 dpa.	3 dpa.
5-7 dpa.	4 -6 dpa
18dpa	8 – 12 dpa
39dpa	16 dpa

As far as the early stages are concerned (0-3 days pa), the overall microscopic analysis of the explant regeneration shows a complex of processes and a series of involved structures that, in terms of morphology, histology and growth rate are closely related to those described in the normal arm regeneration of *A. filiformis*. In fact, the explant response to the injury appears to be effective as that of the normal arm in terms of activation of processes. Since these early stages, even at 1 dpa, the D side, in particular, initiates a real healing process, starting to form a very thin epithelial layer, which covers the wound area. On the other hand, cell mobilization/migration processes are already activated in the coelomic canals, namely in the radial water canal, while the aboral muscle close to the wound starts an extensive reorganization process, showing a progressively more and more disorganized pattern with loss of bundle pattern and integrity and dedifferentiation processes of myocytes. For the remaining time points from 3 days up to 39 days pa, the repair phenomena are followed by typical regeneration processes, the most noticeable general differences seen between explant regeneration and arm regeneration is the delayed time in the explant, expressed in the length and the growth rate of the regenerate following the 3 day stage. In terms of size and morphogenesis the final regenerating arm regrown on the explant is more or less one third that regrown on the normal donor arm. On the basis of our results, it is possible to propose a certain correspondence between the stages described in the two different models. In particular, if 1dpa and 3dpa stages in explant regeneration appear to roughly correspond to 1dpa and 3 dpa stages in arm regeneration, the following stages show a significant delay, 5 dpa and 7 dpa stages in explant corresponding to 4 dpa-6dpa stages in arm regeneration. The delay appear to be more and more pronounced when we compare advanced stages, 18 dpa stage in explant regeneration corresponding to 8 dpa-12 dpa stages in arm regeneration, whereas 39 dpa stage in explant regeneration was comparable to 16 dpa stage in arm regeneration.

In terms of cell recruitment, apart from a basal contribution of new cells apparently derived from proliferation of the coelomic walls, as in many other echinoderm regeneration models (Candia Carnevali, 2005; Garcia-Arraras & Dolmatov, 2010; Garcia-Arraras *et al.*, 1998; Sharlaimova *et al.*, 2014; Sköld & Rosenberg, 1996), muscles play a significant role in regeneration (Garcia-Arraras & Dolmatov, 2010) and even more in explants, since most of the "material" for the outgrowth of the regenerate appear to come from them. On the whole, meaningful contributions in rearrangement of the dedifferentiated myocytes during regeneration observed at the level of the

intervertebral muscles in both arm and explant models are highly analogous and comparable. The participation of dedifferentiated myocytes in the regenerative processes indicates that there is a second important recruitment mechanism involving extensive local phenomena of rearrangement and recycling of the existing arm tissues. The constant presence of groups of dedifferentiating myocytes from the early repair to the advanced regenerative phase in the areas close to the intervertebral muscles of the stump, in the interspaces between muscles and coelomic cavities, and inside the canals themselves (see Fig. 19. d-k, Fig. 20. m-bb), provide strong evidence for the role of dedifferentiated cells. The results in ophiuroid explant samples, in particular, confirm the already discussed evidence of co-existence of epimorphic and morphallactic (Candia Carnevali. & Bonasoro, 2001) processes not only in ophiuroid and in crinoid arm regeneration but in many other organisms and appendages (Dubois & Ameye, 2001) at a cellular level, to provide further good evidence of the plasticity of the prodigious regeneration potential in echinoderms.

Additionally, the directionality of the regenerative process is very clear in explants as demonstrated by our results. Although double amputated at the same time, the explants, in fact, are able to maintain the normal proximal-distal axis of growth. Interestingly, if in the early phases repair and healing phenomena take place at the level of both amputations, proximal and distal, only the distal end undergoes regeneration and regrowth at the advanced stages, whereas the proximal end shows only cicatrization and re-epithelization of the exposed amputation surface. The causes of this different behavior between the proximal and the distal amputations in terms of regenerative potential are far from being well understood in ophiuroids; however, as suggested in crinoids (Candia Carnevali *et al.*, 1998), this difference must be genetically programmed and possibly regulated by differential expression of signal molecules and growth factors that need to be studied in detail.

Overall, if we compare ophiuroid explants with crinoid explants previously studied, we can underline are general similarities in regeneration (Candia Carnevali & Bonasoro, 2001) (Thorndyke *et al.*, 2001) (Candia Carnevali, 2006). Certainly in both groups regeneration involves the development of new structures from migratory presumptive pluripotent cells, which actively proliferate forming a regenerative blastema, and in both cases dedifferentiation phenomena are fundamental. Although preliminary, as far as

arm explants are concerned, the obtained results suggest that, like in crinoid arm regeneration, also in ophiuroids arm regeneration the regenerative potential is strictly based on the remarkable functional autonomy of the arm itself, not only in terms of cells and tissues involved, but also in terms of regulative mechanisms and molecules implied (Burns *et al.*, 2011). Another common aspect is the involvement and crucial role that the nervous system seems to play in echinoderm regenerative development (Garcia-Arriaras *et al.*, 1999) (Franco *et al.*, 2012), confirming the idea of nerve's dependency for regeneration (Candia Carnevali *et al.* 2001), where the developing and regenerating nervous system, particularly the radial nerve cords with all its components and the coelomic plexuses, can interact to a different extent with the mechanisms of epimorphic regeneration (Brookes, 1987; Mashanov *et al.*, 2013). It has been suggested that the contribution of the radial nerve cord during regeneration involves the release of presumptive growth factors demonstrated in some molecular studies of regeneration in terms of identification of growth and neurotrophic factors. Such a role seem to be played by *Afuni* and *afBMP2/4*, recently isolated in *A. filiformis*, suggesting the contribution in controlling arm regeneration in ophiuroids, though their role is still uncertain (Bannister *et al.*, 2008). Other molecules under study, such as SALMFamide 1 (S1) and SALMFamide 2 (S2), have been localized at the nervous tissue (Bremaeker *et al.*, 1997), although there is no proof, at the moment, of any significant involvement in regeneration itself. It is intriguing that some authors suggest that in echinoderms these factors can be considered not only as a “constitutive” neurotrophic factor, but possibly as a broad-spectrum multifunctional regulators of cell proliferation and differentiation which plays a key role during regenerative developmental processes (Candia Carnevali *et al.*, 1998).

4.3. Ophioderma cinerea and Ophioderma appressa.

4.3.1. Morphological analysis

4.3.1.1. Light microscopy

The regenerative process described here with caribbean organisms *O. cinerea* and *O. appressa* and documented by pictures taken under the stereoscope, represent a preliminary work: nevertheless the results obtained so far seem to largely confirm the main general aspects of the regenerative processes described in the present work or

previously described in other ophiuroids (Biressi *et al.*, 2009) in terms of main developmental phases and events.

In terms of representative stages from the early post-autotomic stage up to the development of a miniature functional arm complete in all its anatomical features, the overall regenerative process of *O. cinerea* and *O. appressa* from a morphological point of view, can be preliminary subdivided into the four main phases based on the developmental scheme suggested by (Biressi *et al.*, 2009) as a repair phase, an early regenerative phase, an intermediate regenerative phase and an advanced regenerative phase. This could support the idea of a common regenerative pathway in this group, which, although very versatile and species-specifically plastic, remains uniform in its basic mechanisms and features (Fig 21).

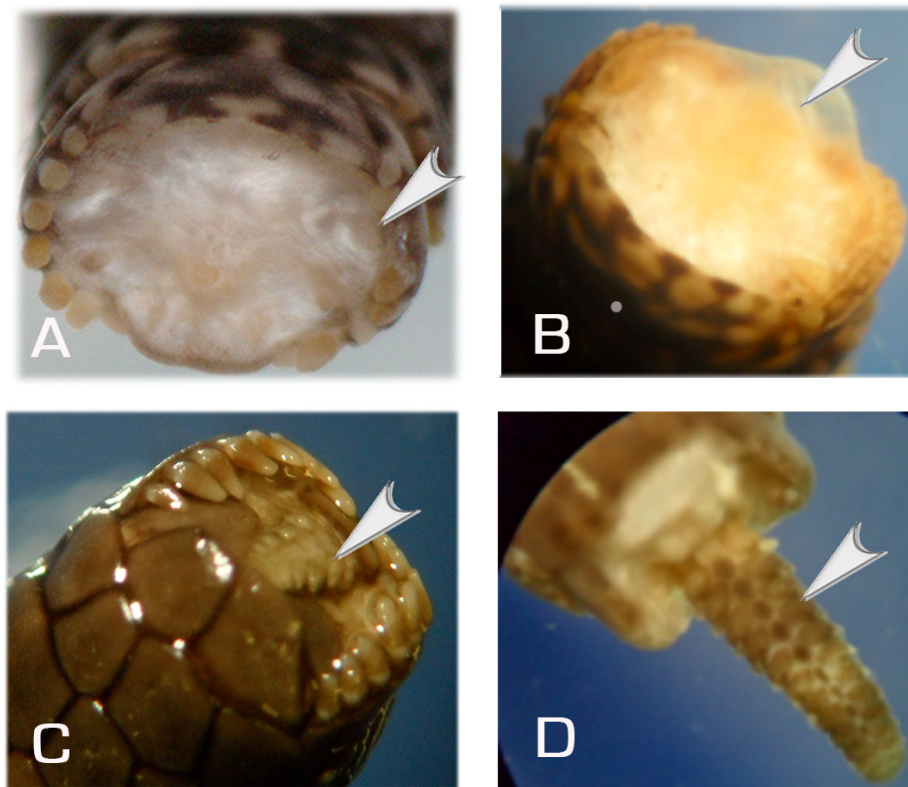


Fig 21. *Ophioderma cinerea*: arm regeneration phases at Stereomicroscope. The main aspects closely correspond to what described in *O. longicauda*. **A.** Repair phase: Amputation surface immediately after natural autotomy. The oral and aboral shields are beginning to bend inwards. **B.** Early regenerative phase: first signs of bud formation are visible in the center of the amputation surface. The growth area is partly protected by the external skeletal shields facing (arrow head) inwards as described in *O. longicauda*. **C.** Intermediate regenerative phase: a miniature regenerative arm more defined in structure is progressively growing (see fig 11 e, f). **D.** Advanced regenerative phase: at 5 to 6 weeks post amputation a longer miniature arm with more defined structures and enhanced external coloration is regrowing from the stump.

4.3.2. Molecular biology preliminary results

Ophioderma appressa.

SoxB1 was successfully clone in *O. appressa*. SoxB1 is involved in the early part of regeneration when undifferentiated cells predominate. It has the ability to maintain neuronal stem cells in an undifferentiated state and actually requires Sox B1 activity to do so (Holmberg *et al.*, 2008). (Holmberg *et al.*, 2008) further demonstrated that SoxB1 can prevent neuronal stem cells from differentiating. A very similar clone to SoxB1 transcription factor has been already detected in *A. filiformis*. Sox1 transcription factors are involved in neuronal determination by preventing undifferentiated cells from terminally differentiation into neurons (Bylund *et al.*, 2003). Because of the importance of the Sox family and the presence of SoxB1 in *O. appressa* it could be hypothesis that this gene could have a regulary input in this specie similar to that aready found in *A. filiformis*.

Conclusions

In this thesis cellular and molecular aspects of the arm regeneration process were explored and compared in both normal arm and explants in different ophiuroid models (brittle stars) at early time points.

In *O. longicauda* the regenerative phenomenon was studied by employing two approaches. The first approach, focused on the development of the regenerate in terms of external and internal microscopic anatomy. This allowed defining crucial aspects of the different stages at early time points and to complete the description of the phenomenon previously provided. At the same time, broadening the knowledge and confirming the classification of its main phases proposed by other authors (Biressi *et al.*, 2009). Overall, the regenerative sequence of morphological events and processes characterizing the arm regeneration at early time points, both the repair and regenerative phenomena, are comparable with those described in other species of ophiuroids already studied (Biressi *et al.*, 2009). This supports the idea of a common regenerative pathway within this group.

The second approach in *O. longicauda* was to identify putative genes with possible implications in regeneration at early time points. Due to the lack of data in molecular biology techniques applied to echinoderms, the positive results of this approach, although preliminary, makes it very promising. *O. longicauda* clones were singled-out, and sequenced. The identified *DNAJC7* cDNA clone was used to perform *in-situ* hybridization (ISH) on the whole animal arm, optimizing and modifying the method for the *O. longicauda* model. In situ hybridization analysis revealed a clear strong expression in the radial water canal system (RWC) of both the freshly cut and the regenerating arm at 24 h and 48 h. This hypothesis 1) further implies a key role for the coelomic RWC as a source of cellular elements for use in ophiuroids arm regeneration as also well demonstrated at histological level in this model (Biressi *et al.*, 2009) and in other echinoderm regeneration models (Candia Carnevali & Bonasoro, 2001; Candia Carnevali *et al.*, 2006; 2009); 2) a specific potential involvement of *DNAJC7 like* in arm regeneration in *O. longicauda*. Further development of techniques for functional gene analysis will certainly enrich the molecular toolbox available for *O. longicauda*, although the results of this study already provide a good starting point for future

research into deuterostomes regeneration and increase our understanding of the evolution and mechanisms of this process.

For the other ophiuroid models used, caribbean related species, *O. cinerea* and *O. appressa*, even though results are only preliminary, provide a comparative view in terms of main developmental phases and events and confirm the main general aspects of the regenerative processes in this important group.

On the other hand, in *A. filiformis* the study was addressed to the explant model, where the different repair and regenerative stages were explored in terms of morphological aspects in both of the amputated explant ends. This results, strongly confirmed in ophiuroids the programmed polarity of the regenerative processes where only the distal end is able to effectively re-grow, whereas the proximal end is undergoing simple repair. These mechanism at cellular and most of all, molecular level, are far from being well understood; however, as suggested in crinoids (Candia Carnevali *et al.*, 1998) this difference must be genetically programmed and possibly regulated by differential expression of signal molecules and growth factors that need to be studied in all their involvement and implications. Hence, since arm explants have shown a remarkable capacity of survival and long-term autonomy (Candia Carnevali *et al.*, 1998) and could be a useful, simple and basic model to investigate elementary influences of the local tissue on regeneration.

Furthermore, in both, arm or explants regeneration, the amputated stump can simply undergo modest repair processes or very complex regenerative ones by employing a few types of progenitor cells (undifferentiated or dedifferentiated) which, through migration, proliferation and differentiation processes associated to appropriate morphogenetic mechanisms, can restore the original morphology of the entire arm in its functional integrity maintaining a directional growth and polarity.

Ophiuroid models use for regeneration studies provide a rich source of inspiration and material for future research where some histological and molecular approaches have already been successfully established. All of these results suggest the importance and

plasticity of these models for regenerative studies providing evidence of the co-existence of epimorphic and morphallactic processes in echinoderm regeneration whose successful effective combination could be considered a reflection of the increase in relevant gene families and responsibility of their amazing regenerative special characteristics. It is probable, in fact, that mechanisms controlling echinoderms regeneration may operate also in chordates, including vertebrates. As a result, ophiuroids have the potential to offer a variety of viable and *tractable models* for a comparative holistic approach to regeneration including molecular, cellular and tissue aspects. For this reason and due to their phylogenetic position closely related to chordates (Ferraz Franco *et al.*, 2014) they offer excellent example of complex and highly evolved organisms on which regeneration studies should be extensively addressed with an expanding potential for *regenerative medicine*.

Acknowledgments

I am grateful with Prof. Daniela Candia for providing valuable knowledge in the echinoderm biology subject, histology and my introduction into the field, also for all the support during my thesis. Thanks to Prof. Luca Del Giacco and Dr. Anna Ghilardi for leading me in the molecular biology part and kindly hosting me in the lab. Thanks to Dr. Olga Martinez and Dr. Sam Dupont for their helpful suggestions with the ISH, their enthusiasm for biology, the unconditional support during this period and the great time spent at Kristineberg. Thanks to Dr. Federico Brown for hosting me in his lab at the University of Los Andes, for his valuable advises and excitement into the field. Thanks to Dr. Orozco for his kind support in the laboratory with the instruments when needed. Thanks to my colleagues, Christiano, Dario, Alice, Cinzia, Michela, Silvia, Arianna and Francesco for their contribution to my work. Thanks to all those that directly or indirectly contributed for the conclusion of this work. I am also grateful for the PhD funding award provided by the *Università degli studi di Milano (UNIMI)*. Thanks to ASSEMBLE: Association of European marine biological laboratories for the three months full award at the Sven Lovén Centre for Marine Sciences – Kristineberg.

References

- Alers, J. C., Krijtenburg, P.-J., Vissers, K. J., & van Dekken, H. (1999). Effect of bone decalcification procedures on DNA in situ hybridization and comparative genomic hybridization: EDTA is highly preferable to a routinely used acid decalcifier. *Journal of Histochemistry & Cytochemistry*, 47(5), 703-709.
- Angius, D., Wang, H., Spinner, R. J., Gutierrez-Cotto, Y., Yaszemski, M. J., & Windebank, A. J. (2012). A systematic review of animal models used to study nerve regeneration in tissue-engineered scaffolds. *Biomaterials*, 33(32), 8034-8039.
- Aronson, R. B. (1987). Predation of fossil and recent ophiuroids. *Paleobiology*, 13(2), 187-192.
- Aronson, R. B. (1992). Biology of a scale-independent predator-prey interaction. *Marine ecology progress series. Oldendorf*, 89(1), 1-13.
- Atkinson, P. J., Wise, A. K., Flynn, B. O., Nayagam, B. A., & Richardson, R. T. (2014). Hair cell regeneration after ATOH1 gene therapy in the cochlea of profoundly deaf adult guinea pigs. *PloS one*, 9(7), e102077.
- Bannister, R., McGonnell, I. M., Graham, A., Thorndyke, M. C., & Beesley, P. W. (2008). Coelomic expression of a novel bone morphogenetic protein in regenerating arms of the brittle star *Amphiura filiformis*. *Dev Genes Evol*, 218(1), 33-38. doi: 10.1007/s00427-007-0193-9
- Becker, J., & Craig, E. A. (1994). Heat shock proteins as molecular chaperones. *European Journal of Biochemistry*, 219(1-2), 11-23.
- Bement, W. M., Mandato, C. A., & Kirsch, M. N. (1999). Wound-induced assembly and closure of an actomyosin purse string in *Xenopus* oocytes. *Current Biology*, 9(11), 579-587.
- Ben Khadra, Y., Said, K., Thorndyke, M., & Martinez, P. (2014). Homeobox genes expressed during echinoderm arm regeneration. *Biochem Genet*, 52(3-4), 166-180. doi: 10.1007/s10528-013-9637-2
- Biressi, A. C. M., Zou, T., Dupont, S., Dahlberg, C., Di Benedetto, C., Bonasoro, F., . . . Candia Carnevali, M. D. (2009). Wound healing and arm regeneration in *Ophioderma longicaudum* and *Amphiura filiformis* (Ophiuroidea, Echinodermata): comparative morphogenesis and histogenesis. *Zoomorphology*, 129(1), 1-19. doi: 10.1007/s00435-009-0095-7
- Blake, D. B. (1990). Adaptive zones of the class Asteroidea (Echinodermata). *Bulletin of Marine Science*, 46(3), 701-718.
- Bremaeker, N. D., Deheyn, D., Thorndyke, M. C., Baguet, F., & Mallefet, J. (1997). Localization of S1- and S2-like immunoreactivity in the nervous system of the brittle star *Amphipholis squamata* (Delle Chiaje 1828). *Proceedings of the Royal Society of London. Series B: Biological Sciences*, 264(1382), 667-674.
- Brockes, J. P. (1987). The nerve dependence of amphibian limb regeneration. *J Exp Biol*, 132, 79-91.
- Brockes, J. P., & Kumar, A. (2005). Appendage regeneration in adult vertebrates and implications for regenerative medicine. *Science*, 310(5756), 1919-1923.
- Brockes, J. P., & Kumar, A. (2008). Comparative aspects of animal regeneration. *Annu Rev Cell Dev Biol*, 24, 525-549. doi: 10.1146/annurev.cellbio.24.110707.175336
- Brockes, J. P., Kumar, A., & Velloso, C. P. (2001). Regeneration as an evolutionary variable. *J Anat*, 199(1-2), 3-11.
- Buchner, J. (1996). Supervising the fold: functional principles of molecular chaperones. *The FASEB Journal*, 10(1), 10-19.

- Burns, G., Ortega-Martinez, O., Thorndyke, M. C., Peck, L. S., Dupont, S., & Clark, M. S. (2011). Dynamic gene expression profiles during arm regeneration in the brittle star *Amphiura filiformis*. *Journal of Experimental Marine Biology and Ecology*, *407*(2), 315-322. doi: 10.1016/j.jembe.2011.06.032
- Burton, P. M., & Finnerty, J. R. (2009). Conserved and novel gene expression between regeneration and asexual fission in *Nematostella vectensis*. *Dev Genes Evol*, *219*(2), 79-87. doi: 10.1007/s00427-009-0271-2
- Bylund, M., Andersson, E., Novitch, B. G., & Muhr, J. (2003). Vertebrate neurogenesis is counteracted by Sox1-3 activity. *Nature neuroscience*, *6*(11), 1162-1168.
- Callis, G., & Sterchi, D. (1998). Decalcification of bone: Literature review and practical study of various decalcifying agents. Methods, and their effects on bone histology. *Journal of histotechnology*, *21*(1), 49-58.
- Candia Carnevali, Bonasoro, F., Patrino, M., & Thorndyke, M. C. (1998). Cellular and molecular mechanisms of arm regeneration in crinoid echinoderms: the potential of arm explants. *Dev Genes Evol*, *208*(8), 421-430.
- Candia Carnevali, M., Galassi, S., Bonasoro, F., Patrino, M., & Thorndyke, M. (2001). Regenerative response and endocrine disrupters in crinoid echinoderms: arm regeneration in *Antedon mediterranea* after experimental exposure to polychlorinated biphenyls. *J Exp Biol*, *204*(Pt 5), 835-842.
- Candia Carnevali, M. D. (2005). Regenerative response and endocrine disrupters in crinoid echinoderms: an old experimental model, a new ecotoxicological test. *Prog Mol Subcell Biol*, *39*, 167-200.
- Candia Carnevali, M. D., & Bonasoro, F. (2001). Introduction to the biology of regeneration in echinoderms. *Microsc Res Tech*, *55*(6), 365-368. doi: 10.1002/jemt.1184
- Carlson, B. M. (2005). Some principles of regeneration in mammalian systems. *The Anatomical Record Part B: The New Anatomist*, *287*(1), 4-13.
- Candia Carnevali, MD. (2006). Regeneration in Echinoderms: repair, regrowth, cloning. *Invertebrate Surviv J*, *3*(1), 64-76.
- Chia, F.-S., & Xing, J. (1996). Echinoderm coelomocytes. *Zoological studies-taipei*, *35*, 231-254.
- Connolly, S., Trevett, A. J., Nwokolo, N. C., Lalloo, D. G., Naraqi, S., Mantle, D., . . . Warrell, D. A. (1995). Neuromuscular effects of Papuan Taipan snake venom. *Annals of neurology*, *38*(6), 916-920.
- Cuénot, L. (1948). Anatomie, éthologie et systématique des échinodermes. *Traité de zoologie*, *11*, 1-363.
- Davidson, E. H., Cameron, R. A., & Ransick, A. (1998). Specification of cell fate in the sea urchin embryo: summary and some proposed mechanisms. *Development*, *125*(17), 3269-3290.
- Detrait, E., Eddleman, C. S., Yoo, S., Fukuda, M., Nguyen, M. P., Bittner, G. D., & Fishman, H. M. (2000). Axolemmal repair requires proteins that mediate synaptic vesicle fusion. *Journal of neurobiology*, *44*(4), 382-391.
- Diachenko, L., Lau, Y. F. C., Campbell, A. P., Chenchik, A., Mogadam, F., Huang, B., . . . Sverdlov, E. D. (1996). Suppression Subtractive Hybridization: A method for generating differentially regulated or tissue-specific cDNA probes and libraries. *Proc. Natl. Acad. Sci*, *93*(12), 6025-6030.
- Diatchenko, L., Lukyanov, S., Lau, Y.-F. C., & Siebert, P. D. (1999). [20] Suppression subtractive hybridization: A versatile method for identifying differentially expressed genes. *Methods in enzymology*, *303*, 349-380.

- Donaldson, D. J., Mahan, J. T., Hasty, D. L., McCarthy, J. B., & Furcht, L. T. (1985). Location of a fibronectin domain involved in newt epidermal cell migration. *J Cell Biol*, *101*(1), 73-78.
- Dubois, P., & Ameye, L. (2001). Regeneration of spines and pedicellariae in echinoderms: a review. *Microsc Res Tech*, *55*(6), 427-437. doi: 10.1002/jemt.1188
- Elangovan, S., Avila-Ortiz, G., Johnson, G. K., Karimbux, N., & Allareddy, V. (2013). Quality assessment of systematic reviews on periodontal regeneration in humans. *Journal of periodontology*, *84*(2), 176-185.
- Emson, R. H., & Wilkie, I. C. (1980). *Fission and autotomy in echinoderms*: Aberdeen University Press.
- Ferraz Franco, C., Santos, R., & Varela Coelho, A. (2014). Proteolytic events are relevant cellular responses during nervous system regeneration of the starfish *Marthasterias glacialis*. *J Proteomics*, *99*, 1-25. doi: 10.1016/j.jprot.2013.12.012
- Franco, C. F., Soares, R., Pires, E., Santos, R., & Coelho, A. V. (2012). Radial nerve cord protein phosphorylation dynamics during starfish arm tip wound healing events. *Electrophoresis*, *33*(24), 3764-3778. doi: 10.1002/elps.201200274
- Gage, J. D. (1990). Skeletal growth bands in brittle stars: microstructure and significance as age markers. *Journal of the Marine Biological Association of the United Kingdom*, *70*(01), 209-224.
- Galko, M. J., & Krasnow, M. A. (2004). Cellular and genetic analysis of wound healing in *Drosophila* larvae. *PLoS biology*, *2*(8), e239.
- Garcia-Arraras, J. E., Diaz-Miranda, L., Torres, II, File, S., Jimenez, L. B., Rivera-Bermudez, K., Cruz, W. (1999). Regeneration of the enteric nervous system in the sea cucumber *Holothuria glaberrima*. *J Comp Neurol*, *406*(4), 461-475.
- Garcia-Arraras, J. E., & Dolmatov, I. Y. (2010). Echinoderms: potential model systems for studies on muscle regeneration. *Curr Pharm Des*, *16*(8), 942-955.
- Garcia-Arraras, J. E., Estrada-Rodgers, L., Santiago, R., Torres, II, Diaz-Miranda, L., & Torres-Avillan, I. (1998). Cellular mechanisms of intestine regeneration in the sea cucumber, *Holothuria glaberrima* Selenka (Holothuroidea:Echinodermata). *J Exp Zool*, *281*(4), 288-304.
- Gierer, A., Berking, S., Bode, H., David, C. N., Flick, K., Hansmann, G., Trenkner, E. (1972). Regeneration of hydra from reaggregated cells. *Nature/New Biology*, *239*(88), 98-101.
- Goss, Custard, J. (1969). The winter feeding ecology of the Redshank *Tringa totanus*. *Ibis*, *111*(3), 338-356.
- Hayward, P. J., & Ryland, J. S. (1990). *Marine fauna of the British Isles and North-West Europe*.
- Hernroth, B., Farahani, F., Brunborg, G., Dupont, S., Dejmek, A., & Skold, H. N. (2010). Possibility of mixed progenitor cells in sea star arm regeneration. *J Exp Zool B Mol Dev Evol*, *314*(6), 457-468. doi: 10.1002/jez.b.21352
- Hohenstein, B., Kasperek, L., Kobelt, D.-J., Daniel, C., Gambaryan, S., Renné, T., Hugo, C. P. M. (2005). Vasodilator-Stimulated Phosphoprotein-Deficient Mice Demonstrate Increased Platelet Activation but Improved Renal Endothelial Preservation and Regeneration in Passive Nephrotoxic Nephritis. *Journal of the American Society of Nephrology*, *16*(4), 986-996. doi: 10.1681/asn.2004070591
- Holmberg, J., Hansson, E., Malewicz, M., Sandberg, M., Perlmann, T., Lendahl, U., & Muhr, J. (2008). SoxB1 transcription factors and Notch signaling use distinct mechanisms to regulate proneural gene function and neural progenitor differentiation. *Development*, *135*(10), 1843-1851.

- Hyman, L. H. (1955). The invertebrates: Echinodermata, the coelomate Bilateria. McGraw-Hill; 1st edition
- Joanna Aizenberg, A. T., Steve Weiner, Lia Addadi & Gordon Hendler. (2001). Calcitic microlenses as part of the photoreceptor system in brittlestars. *Nature* 412, 819-822.
- King, R. S., & Newmark, P. A. (2012). The cell biology of regeneration. *J Cell Biol*, 196(5), 553-562. doi: 10.1083/jcb.201105099
- Kularatne, S. A. M. (2002). Common krait (*Bungarus caeruleus*) bite in Anuradhapura, Sri Lanka: a prospective clinical study, 1996–98. *Postgraduate Medical Journal*, 78(919), 276-280. doi: 10.1136/pmj.78.919.276
- Kurdziel, J. P., Clements, L.A.J., Bell, S.S. (1994). Abundance and arm loss of the infaunal brittlestar *Ophiophragmus filigraneus* (Echinodermata: Ophiuroidea), with an experimental determination of regeneration rates in natural and planted seagrass beds. *Marine Biology*. 121(1), 97-104 . doi 10.1007%2Fb00349478
- Lawrence, J. M. (2010). Energetic costs of loss and regeneration of arms in stellate echinoderms. *Integr Comp Biol*, 50(4), 506-514. doi: 10.1093/icb/icq027
- Lin, F., Zhu, J., Tonnesen, M. G., Taira, B. R., McClain, S. A., Singer, A. J., & Clark, R. A. F. (2014). Fibronectin peptides that bind PDGF-BB enhance survival of cells and tissue under stress. *Journal of Investigative Dermatology*, 134(4), 1119-1127.
- Mashanov, V. S., Zueva, O. R., & Garcia-Ararras, J. E. (2013). Radial glial cells play a key role in echinoderm neural regeneration. *BMC Biol*, 11(49), 1-18. doi: 10.1186/1741-7007-11-49
- Matranga, V., Pinsino, A., Celi, M., Di Bella, G., & Natoli, A. (2006). Impacts of UV-B radiation on short-term cultures of sea urchin coelomocytes. *Marine Biology*, 149(1), 25-34.
- Muller, J., & Troschel, F. H. (1842). System der Asteriden. 1. Asteridae. 2. Ophiuridae. *Archiv filr Naturgeschichte*, 8, 1-134.
- Ockelmann, K. W., & Muus, K. (1978). The biology, ecology and behaviour of the bivalve *Mysella bidentata* (Montagu). *Ophelia*, 17(1), 1-93.
- Parcellier, A., Gurbuxani, S., Schmitt, E., Solary, E., & Garrido, C. (2003). Heat shock proteins, cellular chaperones that modulate mitochondrial cell death pathways. *Biochem Biophys Res Commun*, 304(3), 505-512.
- Patrino, M., McGonnell, I., Graham, A., Beesley, P., Candia Carnevali, M. D., & Thorndyke, M. (2003). Anbmp2/4 is a new member of the transforming growth factor-beta superfamily isolated from a crinoid and involved in regeneration. *Proc Biol Sci*, 270(1522), 1341-1347. doi: 10.1098/rspb.2003.2367
- Patrino, M., Thorndyke, M. C., Candia Carnevali, M. D., Bonasoro, F., & Beesley, P. (2001). Changes in Ubiquitin Conjugates and Hsp72 Levels During Arm Regeneration in Echinoderms. *Marine Biotechnology*, 3(1), 4-15. doi: 10.1007/s101260000018
- Pinsino, A., Thorndyke, M. C., & Matranga, V. (2007). Coelomocytes and post-traumatic response in the common sea star *Asterias rubens*. *Cell stress & chaperones*, 12(4), 331.
- Pula, G., & Krause, M. (2008). Role of Ena/VASP proteins in homeostasis and disease *Protein-Protein Interactions as New Drug Targets* (pp. 39-65): Springer.
- Reimschuessel, R. (2001). A fish model of renal regeneration and development. *Ilar Journal*, 42(4), 285-291.
- Sanchez Alvarado, A. (2000). Regeneration in the metazoans: why does it happen? *Bioessays*, 22(6), 578-590. doi: 10.1002/(sici)1521-1878(200006)22:6<578::aid-bies11>3.0.co;2-#

- Sánchez Alvarado, A. (2004). Regeneration and the need for simpler model organisms. *Philosophical Transactions of the Royal Society of London. Series B: Biological Sciences*, 359(1445), 759-763.
- Say, T. (1825). On the species of the Linnean genus *Asterias* inhabiting the coast of the United States. *Journal of the Academy of natural sciences of Philadelphia*, 5(Part 1), 141-154.
- Sea Urchin Genome Sequencing, C., Sodergren, E., Weinstock, G. M., Davidson, E. H., Cameron, R. A., Gibbs, R. A., ... Wright, R. (2006). The genome of the sea urchin *Strongylocentrotus purpuratus*. *Science*, 314(5801), 941-952. doi: 10.1126/science.1133609
- Seifert, A. W., Kiama, S. G., Seifert, M. G., Goheen, J. R., Palmer, T. M., & Maden, M. (2012). Skin shedding and tissue regeneration in African spiny mice (*Acomys*). *Nature*, 489(7417), 561-565.
- Sharlaimova, N., Shabelnikov, S., & Petukhova, O. (2014). Small coelomic epithelial cells of the starfish *Asterias rubens* L. that are able to proliferate in vivo and in vitro. *Cell Tissue Res*, 356(1), 83-95. doi: 10.1007/s00441-013-1766-8
- Sköld, M., & Rosenberg, R. (1996). Arm regeneration frequency in eight species of Ophiuroidea (Echinodermata) from European sea areas. *Journal of Sea Research*, 35(4), 353-362.
- Slotkin, R. K., & Martienssen, R. (2007). Transposable elements and the epigenetic regulation of the genome. *Nature Reviews Genetics*, 8(4), 272-285.
- Smith, V. J. (1981). The echinoderms. *Invertebrate blood cells*, 2, 513-562.
- Speman, H. (1938). Embryonic development and induction. *The American Journal of the Medical Sciences*, 196(5), 738.
- Stancyk, S. E., Golde, H. M., Pape-Lindstrom, P. A., & Dobson, W. E. (1994). Born to lose. I. Measures of tissue loss and regeneration by the brittlestar *Microphiopholis gracillima* (Echinodermata: Ophiuroidea). *Marine Biology*, 118(3), 451-462.
- Stocum, D. L. (2002). Regenerative biology and medicine. *Journal of musculoskeletal & neuronal interactions*, 2(3), 270-273.
- Storch, V., Welsch, U., & Remane, A. (2005). *Kurzes Lehrbuch der Zoologie*: Elsevier, Spektrum, Akad. Verlag.
- Tawk, M., Joulie, C., & Vríz, S. (2000). Zebrafish Hsp40 and Hsc70 genes are both induced during caudal fin regeneration. *Mech Dev*, 99(1-2), 183-186.
- Tettamanti, G., Grimaldi, A., Congiu, T., Perletti, G., Raspanti, M., Valvassori, R., & Eguileor, M. (2005). Collagen reorganization in leech wound healing. *Biology of the Cell*, 97(7), 557-568.
- Thorndyke, M. C., & Carnevali, M. D. C. (2001). Regeneration neurohormones and growth factors in echinoderms. *Canadian Journal of Zoology*, 79(7), 1171-1208. doi: 10.1139/cjz-79-7-1171
- Thorndyke, M. C., Chen, W. C., Beesley, P. W., & Patruno, M. (2001). Molecular approach to echinoderm regeneration. *Microsc Res Tech*, 55(6), 474-485. doi: 10.1002/jemt.1192
- Thorndyke, M. C., Patruno, M., Chen, W. C., & Beesley, P. W. (2000). *Stem cells and regeneration in invertebrate Deuterostomes*. Paper presented at the Symposia of the Society for Experimental Biology.
- Wadman, M. (2005). Scar prevention: the healing touch. *Nature*, 436(7054), 1079-1080.
- Weissman, I. L. (2000). Stem cells: units of development, units of regeneration, and units in evolution. *Cell*, 100(1), 157-168.
- Wilkie, I. C. (2001). Autotomy as a prelude to regeneration in echinoderms. *Microsc Res Tech*, 55(6), 369-396. doi: 10.1002/jemt.1185

- Wolf, J. H., Bhatti, T. R., Fouraschen, S., Chakravorty, S., Wang, L., Kurian, S., Levine, M. H. (2014). Heat shock protein 70 is required for optimal liver regeneration after partial hepatectomy in mice. *Liver Transpl*, 20(3), 376-385. doi: 10.1002/lt.23813
- Yokoyama, H. (2008). Initiation of limb regeneration: the critical steps for regenerative capacity. *Dev Growth Differ*, 50(1), 13-22. doi: 10.1111/j.1440-169X.2007.00973.x
- Zhu, Y. Y., Machleder, E. M., Chenchik, A., Li, R., & Siebert, P. D. (2001). Reverse transcriptase template switching: A SMART™ approach for full-length cDNA library construction. *Biotechniques*, 30(4), 892-897.